APPENDICES

ADAK ISLAND, ALASKA

MICROEARTHQUAKE SURVEY:

Preliminary Hypocenter Determinations

by

Arthur L. Lange & Walter Avramenko

Subcontract for

Earth Science Laboratory

University of Utah Research Institute

U.S. Department of Energy

Contract No. DE-AC07-80ID12079

5 November 1982

Arthur L. Lange,
Manager

MINCOMP

EXPLORATION RESOURCES

4175 Harlan Street
Wheat Ridge, Colorado
80033

Frontispiece

A) Andrew Bay, Adak Island. Hot Springs are reached by
   following beach around rocky point.

B) Andrew Bay Volcano, with Mt Adagdak in distance.
   Andrew Lake in foreground.

TABLE OF CONTENTS

PART I

MICROEARTHQUAKES AND GEOTHERMAL ACTIVITY: OBSERVATIONS AND PRINCIPLES

PART II

ADAK MICROEARTHQUAKE SURVEY AND RESULTS

APPENDICES

FIGURES

TABLES

FIGURES

TABLE

ABSTRACT

Microearthquakes, defined as shocks having magnitudes less than 4, are commonly recorded in the vicinity of geothermal manifestations and volcanism. They have been mapped from producing geothermal fields as well as those not yet developed, in such places as Iceland, El Salvador, Japan, Kenya and the United States. Microearthquakes have been recorded at several geothermal sites in the Imperial Valley and Coso Hot Springs, California; Kilbourne Hole, New Mexico; Yellowstone National Park, Wyoming; and The Geysers, California, where there is debate over whether or not the seismicity is induced by steam production. Seismicity occurs around active volcanoes, but appears reduced directly over zones of high temperature or magma, where the depth of the brittle fracture zone is shallow, as over Yellowstone caldera.

In areas of active hydrothermalism, regional stress is likely to be relieved by low-level seismicity rather than occasional large ruptures, owing to the high temperatures, presence of fluids, and crustal weakening due to alteration and fracturing. Active faulting maintains the permeability of the system, which in its absence, might otherwise seal. On the microscopic scale, pore-fluid pressures rise as a result of heating, resulting in the decrease of effective pressure at the pore-mineral boundary. When this effective pressure becomes less than the rock's tensile strength, the pore ruptures; and if it intersects a through-going fracture under hydrostatic pressure can result in a shock detectable on seismographs at the surface. Such a mechanism might also account for the swarms of very small events seen in a number of geothermal areas.

A microearthquake survey was conducted on Adak Island, Alaska for the purpose of identifying seismicity associated with a possible geothermal reservoir. During 30 days of recording in September and October 1982, 190 seismic events were recorded on two or more stations of a nine-station network. Of the total, 33 were of local origin, and of these 24 were locatable. Utilizing a 5km/sec constant velocity earth model, the hypocenters define a structure dipping north-northwestward toward the Bering Sea, beneath Mt Adagdak. Many of the events took place beneath the Adagdak peninsula in an area in which hot springs discharge and where other geophysical evidences suggest a geothermal reservoir.

A similar NNW-dipping fault plane was deduced from a 9-day microearthquake survey conducted in 1974. At that time all of the activity occurred beneath the sea. The projected surface trace lies NNW of that deduced from the present survey.

It is quite likely that the mapped structure and attendant fractures control a hydrothermal system by providing the necessary permeability for maintaining circulation of hot waters within the upper several kilometers of the surface.

Only preliminary analysis of the records fell within the scope of the present project. The work should be supplemented with the application of a locally appropriate earth model, 3D fault-mapping, first-motion studies leading to fault-plane solutions, and computations of event magnitudes.

PART I

Microearthquakes and Geothermal Activity:

Observations and Principles

Microearthquakes are discrete earthquakes having Richter magnitudes too small to be felt on the surface or recorded on large scale seismograph networks. They are roughly defined as having magnitudes less than 4, and generally fall in the range between +2 and -2 (Ward, 1972). For each unit decrease in magnitude there occur roughly 10 times as many events; hence, in seismically active areas microearthquakes are normally many times more prevalent than felt events. Microearthquakes are not to be confused with microseisms, which are a form of more or less continuous background noise, originating from cultural activity and storms at sea, or with "groundnoise" or tremor resulting from geyser and fumarolic activity in geothermal areas. Figure 1 shows some typical microearthquake records, in which the events have a more or less abrupt onset followed by a declining wavetrain or coda.

Worldwide occurrences

As early as 1938, MacGregor, and later Sheperd, et al. (1971) on Montserrat, West Indies correlated increases in heatflow around fumaroles with seismic activity. During the 1960's an association of seismicity with geothermal areas was discovered at a number of places around the world. In Japan, Oki, et al. (1968) and Oki & Hirano (1970) discovered microearthquakes beneath a geothermal zone of Hakone volcano, where more than a million events occurred between 1965 and 1968 (Hagiwara & Iwata (1968). Tobin, et al. (1969) recorded microearthquakes in the vicinity
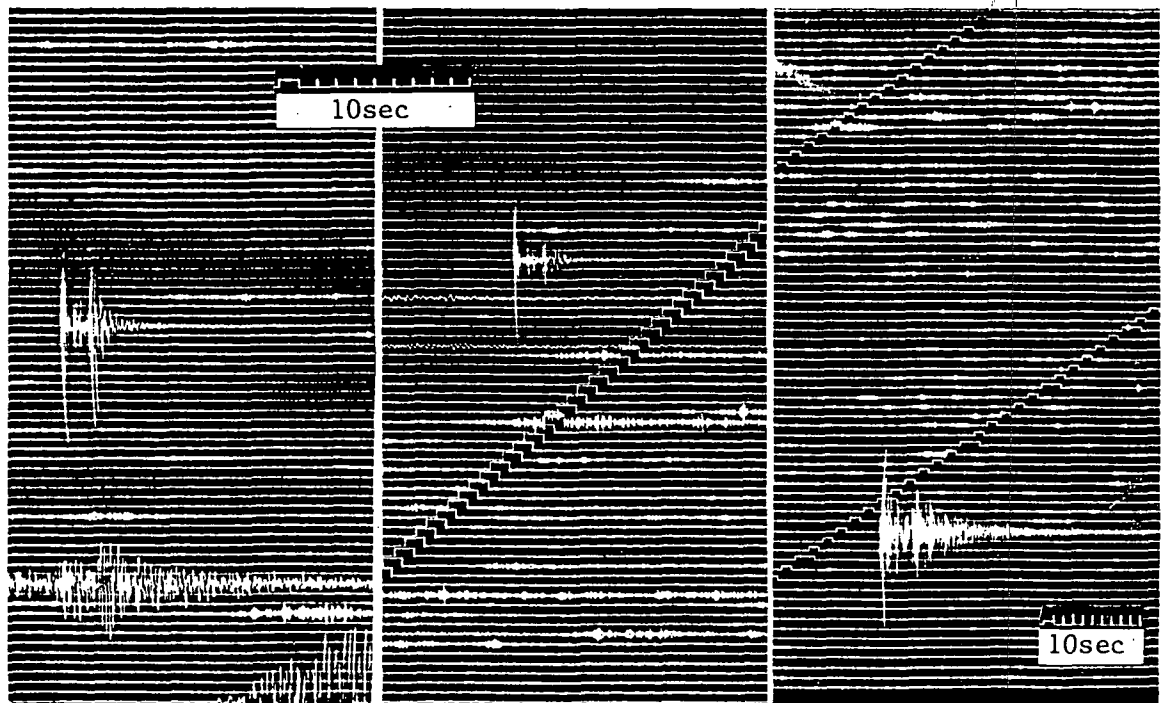
Figure 1. Typical microearthquakes from the vicinity of Mt Adagdak, Adak Island, Alaska. The 13th trace up from the bottom shows an unidentified microseism.
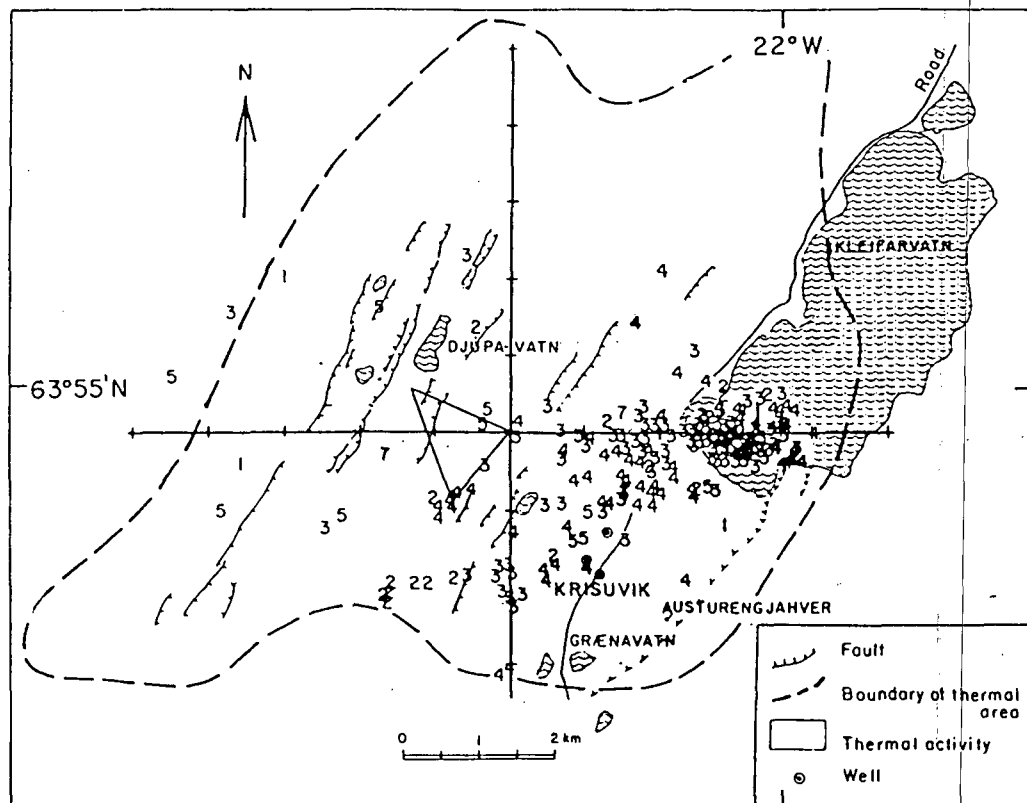
Figure 2. Earthquakes in the Krisuvik geothermal area, 25km SSW of Reykjavik, Iceland. Focal depths shown by numbers (km) and the thermal alteration is outlined by the dashed line (from Ward, 1972).

of geothermal areas around Lakes Naivasha and Magadi in the Rift Valley of Kenya.

In Iceland, Ward, et al. (1969) and Ward & Björnsson (1971) made detailed studies of microearthquakes over geothermal areas (Figure 2). Ward (1972) draws the following conclusions:

1. Most microearthquakes recorded throughout Iceland occurred within or very near major geothermal areas.

2. Geothermal areas that are structurally related to fissure systems generally had microearthquake activity whereas those areas that have few prominent fissures and seem only related to intrusions of silicic magma had little or no microearthquake activity.

3. Epicenters* of microearthquakes in two areas where detailed locations were possible were confined primarily to the region of thermal alteration observed at the surface. The greatest earthquake activity was often near the regions of greatest thermal activity observed at the surface...

*An epicenter is the point on the surface of the earth directly above the hypocenter. The hypocenter is the point in the earth where an earthquake occurs as located with the times of the first seismic arrivals at a number of stations (Ward, 1972).

4. Most well-located microearthquakes in Iceland occurred at depths of 2 to 6km. Some events were as deep as 13km...

5. Operation of a geothermal well, 0.3km deep, did not significantly affect the occurrence of microearthquakes, which were located generally deeper than 2.0km.

6. Earthquakes in geothermal areas in Iceland seem to occur primarily in swarm type sequences whereas earthquakes elsewhere in Iceland occur primarily as mainshock-aftershock sequences. The majority of the seismic energy in a mainshock-aftershock sequence is released during the mainshock. In a swarm sequence, however, the seismic energy is released over a period of as long as days or months during many shocks.

7. Earthquakes with magnitudes greater than 4.5 generally do not seem to be located within geothermal areas, although they may occur only ten or fifteen kilometers away.

An example of microearthquake distribution over the Krisuvik field is shown in Figure 2.

In the Ahuachapan geothermal field, El Salvador, more than 150 local events were recorded during 8 months, for the most part in swarms of 10 to 20 events (Ward & Jacob, 1971). The results are interpreted

Figure 3. Hypocenters projected on a vertical plane, Ahuachapan geothermal area, El Salvador (Ward, 1972).

Figure 4. Epicenters of 17 events in The Geysers' steam field determined from a 6-element array (Lange & Westphal, 1969).

-4-

as an active fault directly under the best producing wells of the field (cf. Figure 3).

These and many other correlations around the world have been compiled along with references in Peter Ward's 1972 paper.

United States occurrences

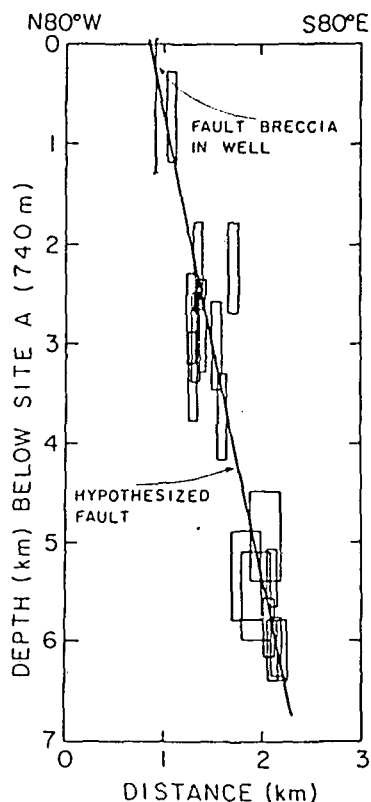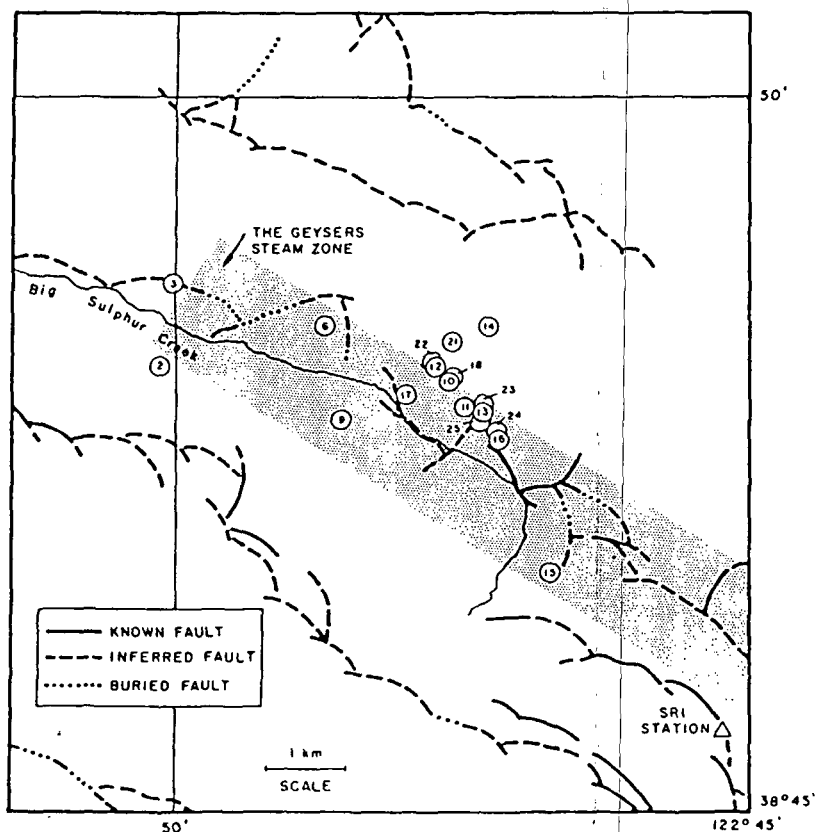Microearthquakes at the Geysers steam zone in northern California were discovered by Lange & Westphal (1969) during a 5-day survey in 1968. All of the activity then recorded took place within the producing zone (Figure 4). The survey was followed up by a more detailed investigation by Hamilton & Muffler (1972) who found that most of the 53 located events occurred in a zone 1km wide by 4km long passing through the principal fault zone of the geothermal field, and within 4km of the surface. Because steam production commenced at the Geysers in 1960, 8 years before the first seismic monitoring, questions have been raised concerning the origin of the seismicity; that is, whether or not it results from steam withdrawal and reinjection, rather that natural processes. Recently, Oppenheimer & Eberhart-Phillips (1982) have reported that prior to the operation of new steam plants in the later extensions of the Geysers field, no seismicity was observed, and that subsequently microearthquakes were observed. Unfortunately, seismographs had not been installed at the new sites until about the time that production began, so that their conclusion that the observed seismicity is almost entirely a result of production may not be universally accepted.

In the Imperial Valley, California, Brune & Allen (1967) mapped abnormally high seismicity south of the Salton Sea, but concluded that they were not solely the result of localized volcanic or thermal activity at depth, but rather resulted from the regional stress associated with the San Andreas fault system. In 1971, however, Thatcher & Brune reported four swarms of earthquakes near Obsidian Buttes geothermal system at the southern end of the Sea.

Jarzabek & Combs (1976) report observing swarms of very small events (M<0) over the Dunes geothermal anomaly on the east side of the Imperial Valley, California. The events occurred at a rate of 20 to 30 per day, often in pairs separated by about 2 seconds.

In the Mesa geothermal anomaly of the Imperial Valley, Combs and Hadley (1977) recorded microearthquakes daily over a period of 5 weeks, but two swarms were observed containing 100 or more small events per day. The seismicity defined a new structure--the Mesa fault--which functions as a conduit for rising geothermal fluids (Figure 5).

Between 5 and 15 events were recorded each day during a 30-day survey around the Kilbourne Hole KGRA, in south-central New Mexico (Johnson & Combs, 1976). Focal depths of 8 to 10km were determined, with epicenters falling primarily along the N/S Fitzgerald fault.

At Coso Hot Springs, Inyo County, California, Combs & Rotstein (1975) detected more than 2000 local events during 33 days of recording. Of the 78 events located, those with focal depths between 1 and 3km clustered around the geothermal manifestations; the deeper events occurred under perlite volcanic domes.
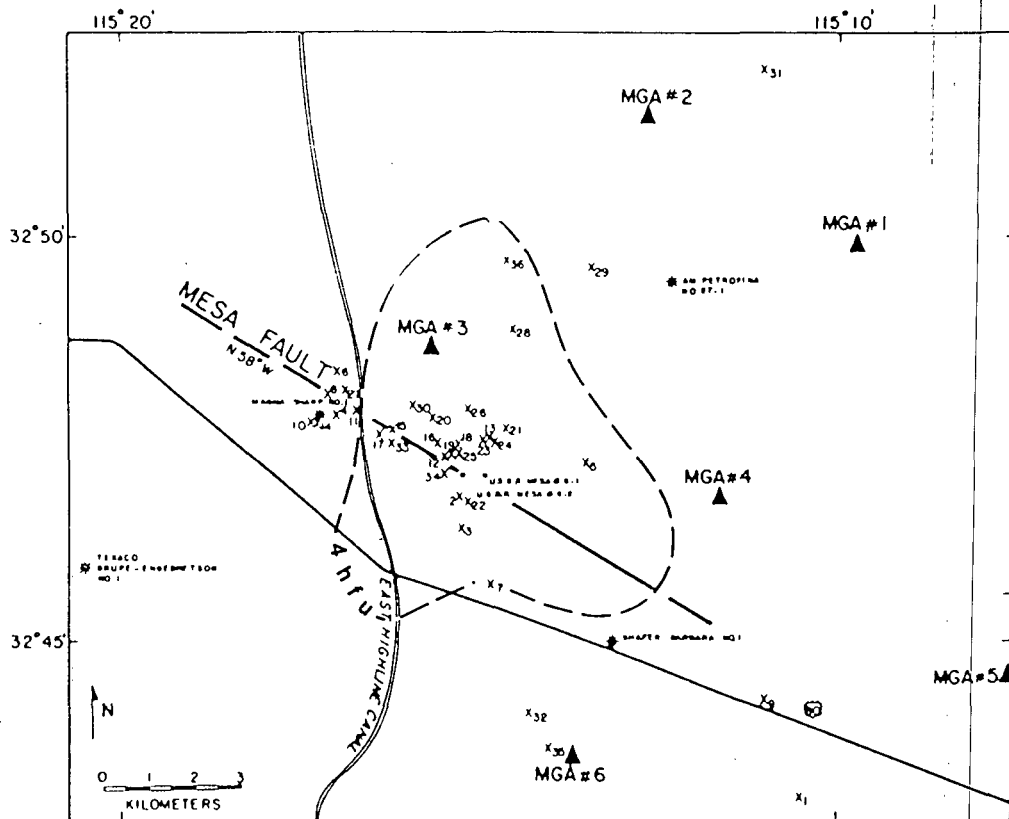
Figure 5. Mesa geothermal anomaly (dashed outline)
   located epicenters (x), and resulting trace of deduced
   fault (from Combs & Hadley, 1977).

Not everywhere is the association between seismicity and geothermal activity immediately obvious. In Yellowstone National Park, Smith, et al. (1977) found a marked decrease in frequency of occurrence within the Yellowstone caldera, compared with structures beyond (Figure 6). Focal depths within the caldera--with one exception--fell above 6km, contrasted with distributions to 20km and deeper outside. They attribute the effect to the limiting depth of brittle fracture within the high-temperature part of the caldera, such that stable sliding occurs at shallow depths.

At Roosevelt Hot Springs, Utah, where electrical power production began in 1981, Olson & Smith (1976) found considerably less seismic activity in the geothermal area relative to the surrounding region. Other workers have reported low-level activity close in to the Hot Spring; A.L. Lange recorded a swarm of local events within a half-kilo-meter of the spring during a 4-day monitoring period in 1976. Here, it may be a matter of detection threshold and proximity to the source. No seismic activity has been observed at the Raft River geothermal development (Schaff, 1981); and to our knowledge no concentrations of seismicity around geothermal areas in the western Snake River plain of Idaho and Oregon have been discovered, possibly due to the attenuating volcanic fill. At Long Valley, California, as at Yellowstone, Steeples & Pitt (1976) found only minor activity inside the caldera, but a high level to the east and south, again probably due to loss of brittle fracture by heating.
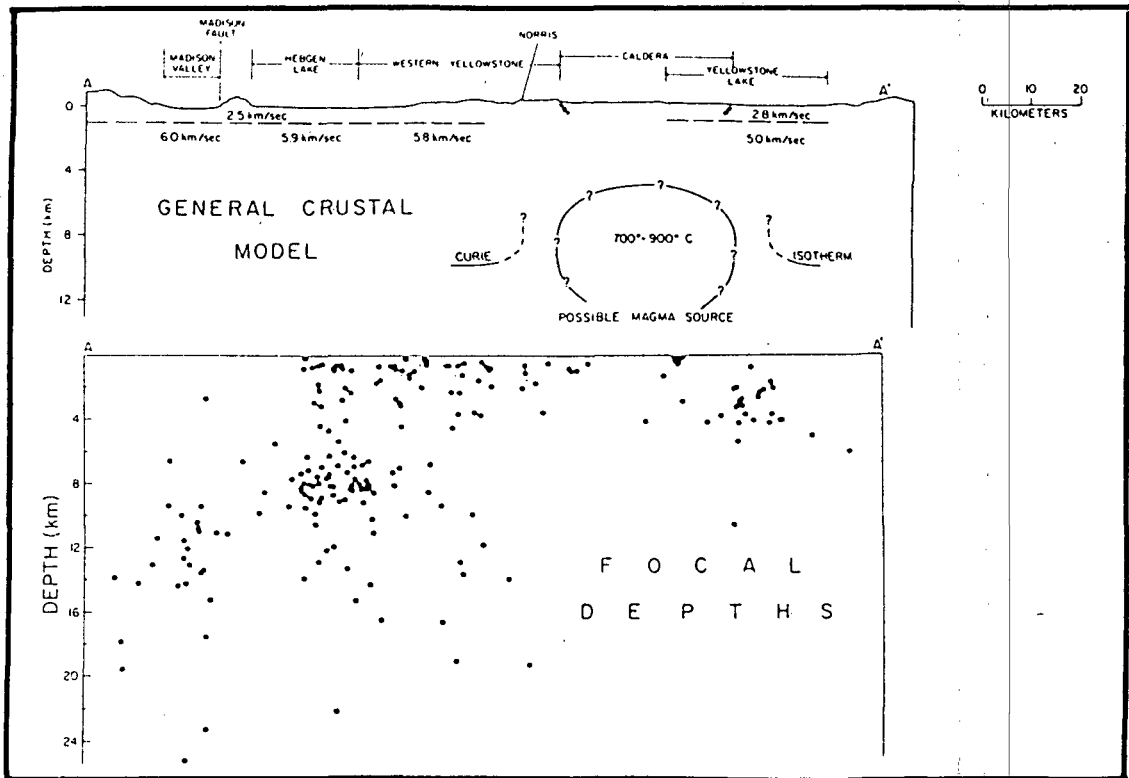
Figure 6. Crustal model for the Yellowstone hot spot
and distribution of earthquake focal depths, showing
reduced incidence beneath caldera (from Smith, et al.,
(1977).

The occurrence of seismic activity associated with volcanic activity
has been well established, and is commonly used to predict eruptions.
Heating and cooling associated with thermal expansion and contraction
around a melt result in considerable cracking. Chouet (1979) reports
that about 8000 small events were recorded per day in 1976 over and
beneath the lava lake of Kilauea Iki, Hawaii. The extensive pipes
of the East rift zone and deeper magma chambers of Kilauea volcano
have been mapped from their seismicity by Ryan, et al. (1981).
In addition, fluid movement transients probably account for the harmonic
tremor activity resembling groundnoise, recorded over volcanoes (Ferrick,
et al., 1982) (Figure 7).
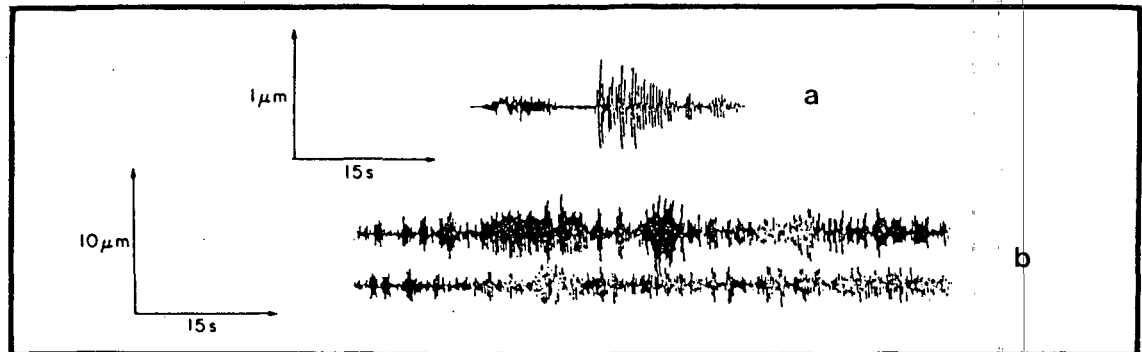
Figure 7. Seismograms from Mt St. Helens, 4 April 1980.
a) Type B volcanic earthquake; b) Two 1-minute segments
from a 20-minute harmonic tremor (from Ferrick, et al.,
1982).
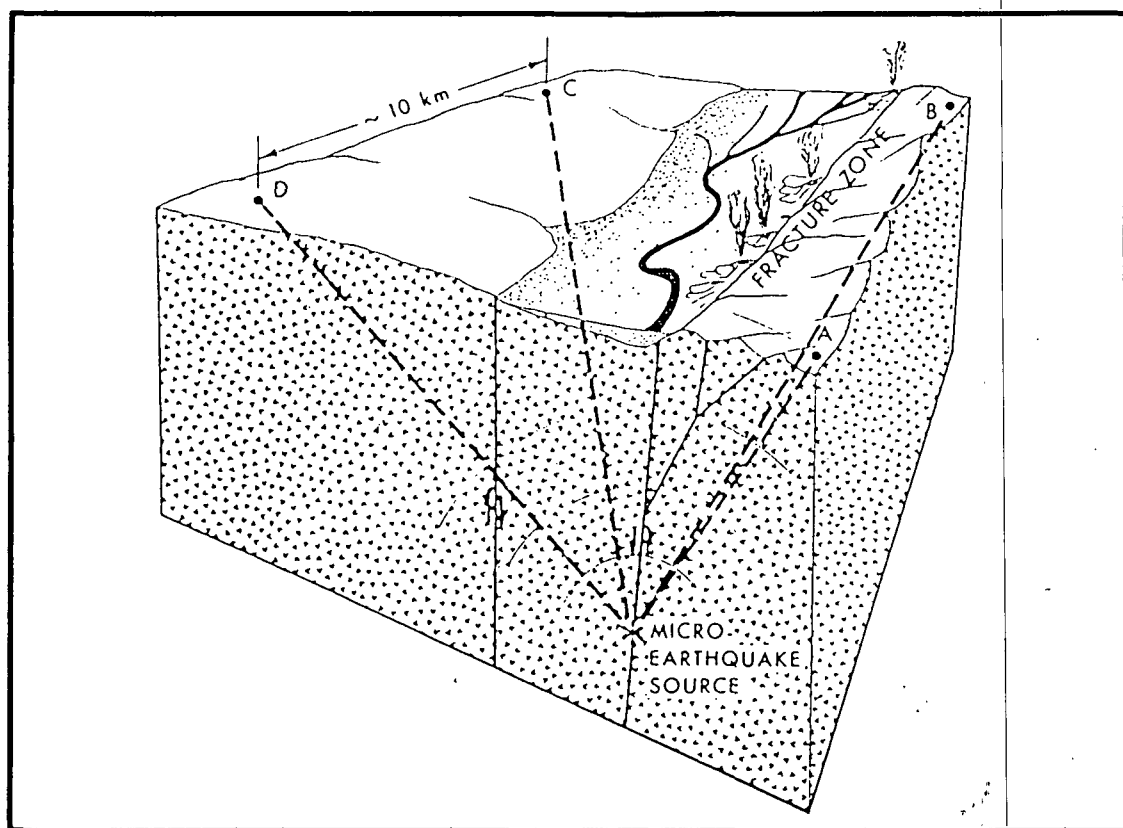
Figure 8. A four-element seismograph network.

Nature of microearthquakes

Microearthquakes in geothermal environments are recorded by an array of seismographs, having station separations between 1 and 10km as discussed in the section on instrumentation (Figure 8). From the differ-ences in arrival times of particular wave phases; for example, the first arrival P-wave, a hypocenter for the event can be computed based on the velocity model adopted. The calculation requires that a common phase be recognized on at least 3 records.

The observed waveforms obtained from vertical seismometers typically have an abrupt P-(compressional) wave arrival, followed by a poorly defined S-(shear) wave arrival superimposed on the coda of the former (Figure 9a). The transverse shear wave is generally much better resolved when horizontal seismometers are employed. Later arrivals such as the Rayleigh, or surface wave, and refracted P and S may appear on records made farther from the source, but they are used more for interpreting than locating.

The S-wave travels slower than the P; hence, the farther from the source, the greater the separation between their arrivals; so that the time difference can be utilized to estimate the distance to the source. Because the ratio of S to P velocities is nearly constant (~0.59) for near-surface rocks,* the time difference between the S and P arrivals,

*Corresponding to a value of 0.235 for Poissons ratio (Gutenberg 1959, p. 165) a representative value for rock near the surface.
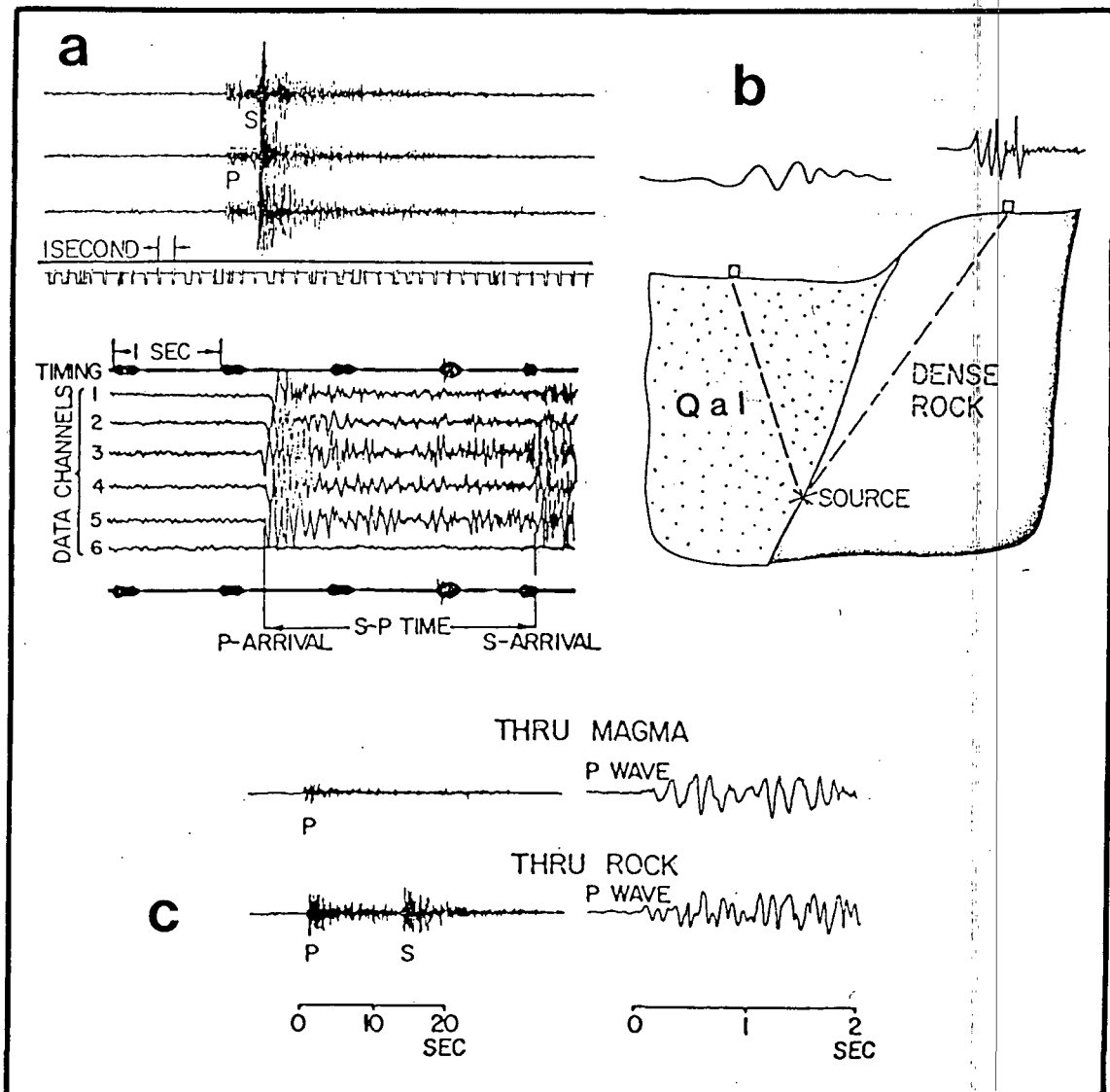
Figure 9. Microearthquake signatures from different environments.
a) P- and S-wave arrivals compressed and expanded from a bedrock
site; b) Comparison of waveforms through alluvium and rock;
c) P- and S-wave attenuations through magma and rock.

T_{sp}, is simply related to the travel time, T_p, of the P wave:

$$T_p = \frac{T_{sp}}{0.7} .$$

If we let w denote the P-wave velocity, the slant range r to the source
is

$$r = w \frac{T_{sp}}{0.7} .$$

A typical P-wave velocity for alluvium is 3km/sec and for granite 6km/sec;
hence, to obtain an estimate of the slant distance, we multiply the S-P
time interval by 4.3 and 8.6, respectively. Of course, changes in
velocity along the travel path may require a model more complex than that
of homogeneous earth.

In Figure 9b, we see the effect of the medium on waveform. Atten-
uation within uncompacted alluvium results in the absorption of higher-
frequency energy and a low-frequency signature at the surface relative
to that seen over dense rock. In addition, the wave is delayed due to
the lower velocity fill. A more extreme case of attenuation occurs
when a seismic wave passes through a magma chamber (Figure 9c). In the
path through the magma, the high frequencies of the P-wave are severely
reduced and the S-wave is completely absorbed, owing to the inability
of a liquid to sustain shear. Examples of seismic waves passing through
the magma chamber beneath Mt Katmai, Alaska are given in Matumoto's
paper (1971). The comparative behavior of P and S-waves through geotherm-
al areas has been utilized to map possible magma chambers (Iyer, et al.,
1978, Eaton, et al., 1975) and reservoir properties (Majer & McEvilly,
1979). Figure 10 illustrates the case of the deduced magma under
Yellowstone caldera.
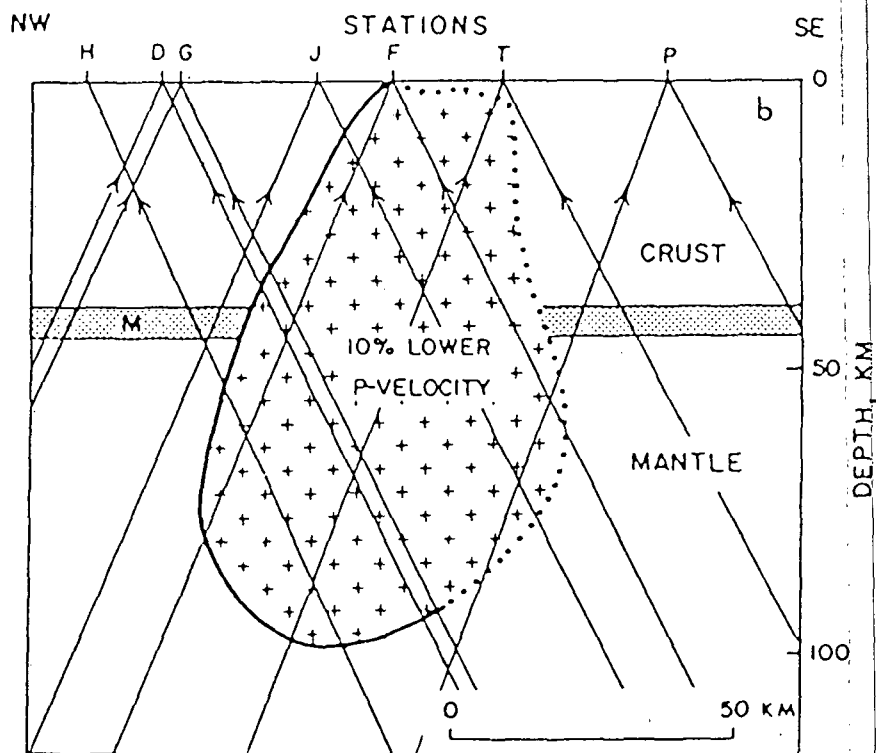
Figure 10. NW-trending vertical cross-section
through the deduced low-velocity medium be-
neath Yellowstone caldera.(Eaton, et al.,
(1975).
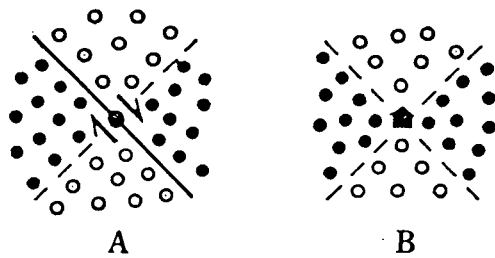
Figure 11. Azimuthal distribution of compression (solid circles) and dilatation (open circles) due to right-lateral strike-slip. A) As observed at points around the epicenter; B) As observed at a station in the center for the epicenters indicated (from Richter, 1958).

Origin of earthquakes

Faulting has long been regarded as the single most important source of earthquakes and led to the "elastic rebound theory" of earthquakes formulated by H.F. Reid, summarized in Richter's (1958) text:

> The energy source for tectonic earthquakes is potential energy stored in the crustal rocks during a long growth of strain. When the accompanying elastic stresses accumulate beyond the competence of the rocks, there is fracture; the distorted blocks snap back toward equilibrium, and this produces the earthquake. Energy is drawn from a wide zone on both sides of the actual fracture. Naturally minor and local shaking may be associated with irregular fault surfaces grinding against each other as fracture progresses and the original process normally continues through a series of aftershocks... Nevertheless, the main features, both macroseismic and microseismic, are best accounted for in terms of a single principal event. Fracture takes place chiefly along already established weaknesses; the great active faults are wounds in the earth which have opened again and again.

In the case of strike-slip faulting, the motion observed at seismographs around the event (Figure 11a) should appear compartmented into quadrants of compression and dilatation. The same effect is expected on one seismograph surrounded by a series of fault epicenters (Figure 11b). Of course, earthquake motion may occur in any attitude resulting in dip-slip and horizontal faulting, leading to more complex portrayals of the fault-plane solution (Stauder, 1962). There remains considerable controversy over the ultimate causes of large earthquakes, as well as fault mechanisms. Likewise, the origin of microearthquakes in geothermal environments has become a subject of much discussion.

Geothermal microearthquakes

In areas of active hydrothermalism, regional stress is likely to be relieved by more or less continuous small earthquake activity, rather than occasional large ruptures, because of the high temperatures, presence of fluids, possibly even magma, and crustal weakening resulting from hydrothermal alteration. Furthermore, the active faulting maintains the permeability required for the meteoric and heated fluids to circulate (Ward, 1972). In the absence of repeated fracturing, the conduits supplying recharge to the system and providing discharge paths to the surface would likely seal, resulting in a "blind" thermal anomaly lacking surface hot springs, fumaroles or geysers.
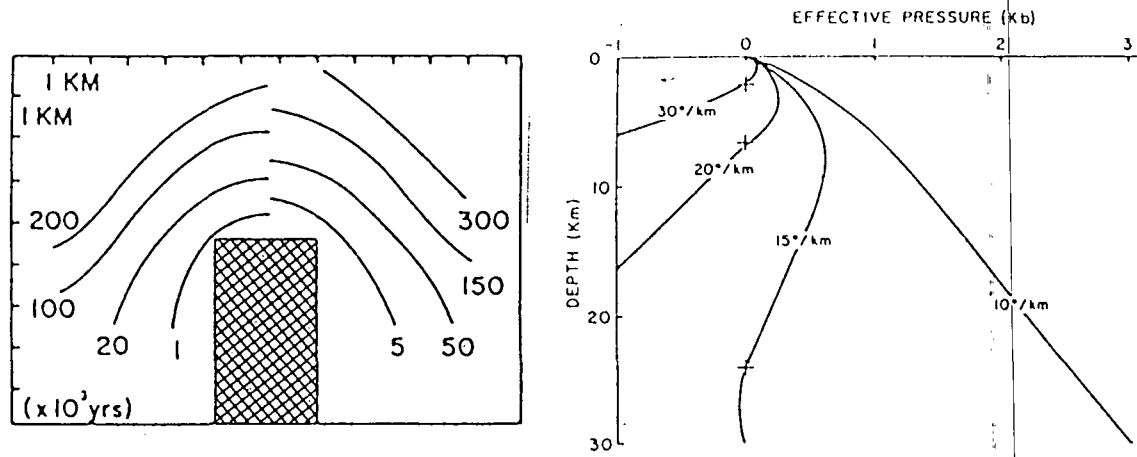
Figure 12. Effect of cooling pluton on effective pressure. A) Iso-
    chrons of zero-effective pressure front; B) Effective pressure
    at depth for various geothermal gradients (Knapp & Knight, 1977).

Knapp & Knight (1977) have investigated the effect of increasing
temperatures of an advancing thermal front on pore-fluid pressures. Their
analysis is applied to the environment of an intruded pluton (Figure 12a)
as well as a hydrothermal system arising from the resultant heating. As
a result of heating, pore-fluid pressures rise, so that the effective
pressure at the pore-mineral boundary decreases (Figure 12b). When
effective pressure becomes less than the tensile strength of the rock,
the isolated pore ruptures, forming a tiny fracture and an inconsequen-
tial shock (Figure 13: Case I). If the fractured pore intersects a
throughgoing fracture under hydrostatic pressure (Case II):

> The pore fluid pressure change in this case can be
> significant, and considerable energy can be released.
> The fracturing of one pore with a volume of 3.4×10^{-9} cm^3
> releases 2×10^{-8}J, which from the Gutenberg-Richter
> equation for surface waves... produces an undetectable
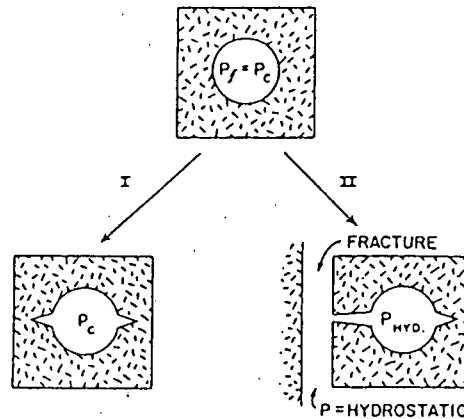
Figure 13. Case I: Rupture of
    isolated pore; Case II: Rupture
    into throughgoing fracture
    (Knapp & Knight, 1977).
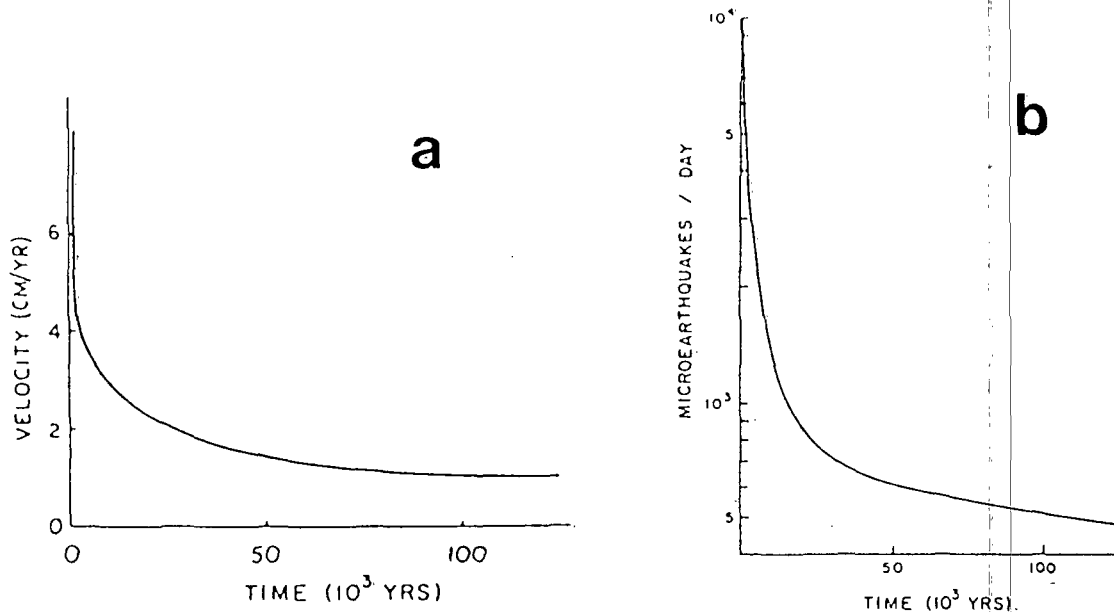
Figure 14. a) Speed of propagation of the zero effective pressure front versus elapsed time for pluton environments; b) Frequency of seismicity (M=0) following emplacement of pluton (Knapp & Knight, 1977).

-7.4 surface wave magnitude microearthquake. A zero magnitude earthquake can be produced if all pores in a cubic meter of rock with a total porosity of 0.01 fracture simultaneously. A 3.6 magnitude earthquake can be produced for 10^{-3} km^3 volume of the same rock.

It is emphasized that the assumption that all pores fracture simultaneously and that energy conversion is 100% efficient is idealized. Simultaneous fracturing is augmented, however, by shock wave propagation. These calculations therefore represent maximums. We also reiterate that the quantitative prediction of pore fluid pressure variations with temperature is only valid before fracturing occurs.

In Figure 14a, Knapp & Knight have shown the speed of propagation of the zero-effective pressure front for the case of an intrusion. The corresponding expected frequency of microearthquake production for events of Magnitude 0 appears in Figure 14b. They note that the incidence of microearthquakes in geothermal areas runs considerably lower than predicted here and account for this as follows:

Clearly, part of this discrepancy is due to the idealized nature of the assumptions that result in the predicted frequencies being maximums. However, the age of the geothermal system must be considered since the theory predicts lower frequencies for increasingly older systems. We therefore suggest that at least some of the micro-earthquakes observed in present-day geothermal systems result from thermally induced hydraulic fracturing of isolated fluid-filled pores. Furthermore, this seismic

activity does not require the presence of a magma body at
depth, since microearthquake production continues after
the pluton is completely crystalline and cooled to nearly
ambient conditions.

The effect of increasing pore-fluid pressures has been demonstrated
during hydraulic stimulation experiments at the hot dry rock site,
Fenton Hill, New Mexico (Pearson, 1981). Several hundred microearth-
quakes of magnitudes between -4 and -2 were recorded.

... These events are probably caused by shear failure
induced by high pore fluid pressures. Since the event
locations seem to cluster in a narrow band near the hydraulic
fracture, we were able to use microseismic techniques to
locate the hydraulic fracture and monitor its growth...

"Typical" geothermal microearthquakes seem to occur in swarms, as
shown in Figure 15, recorded in the Mesa geothermal field by Combs &
Hadley (1977). Called by them nanoearthquakes, these events are of
magnitudes less than zero, and are observed on only one station of the
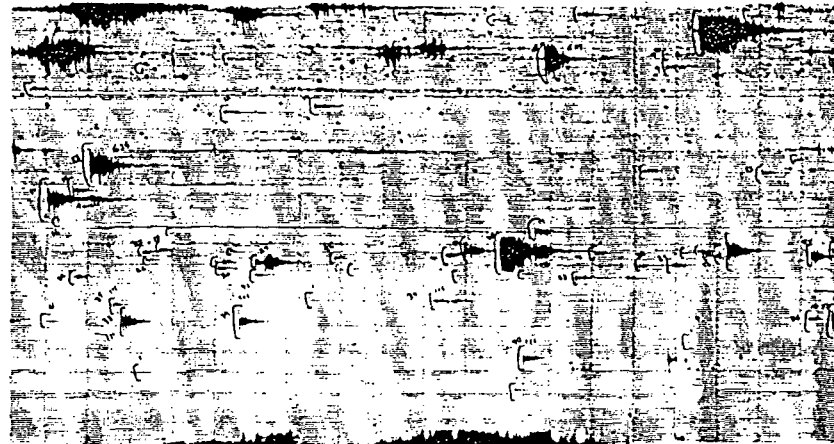
MGA # 3   -30 dB   JUNE 21, 1973   —⊣ ⊢— 20 SEC
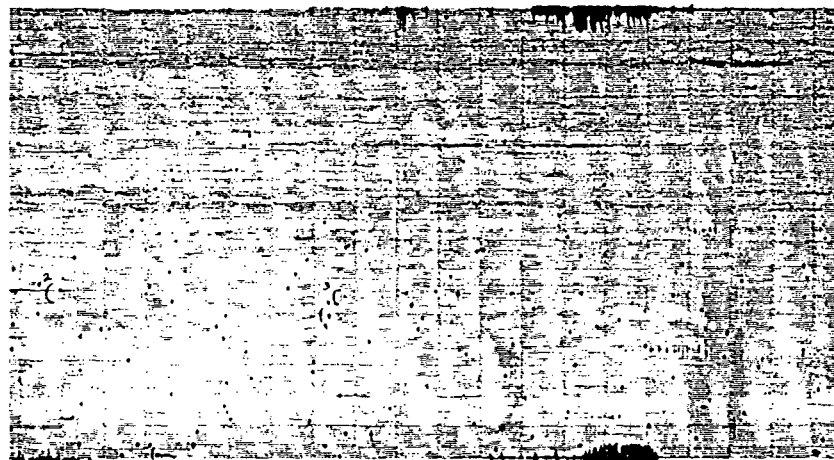
MGA # 3   -30 dB   JULY 12, 1973   —⊣ ⊢— 20 SEC

Figure 15. Micro- and nanoearthquake swarms in
the Mesa geothermal field (Combs & Hadley, 1977).

-14-

net at a rate of at least 100 per day. When a tight array was constructed over the geothermal center, some duplication of events was seen on other stations, but locations could not be obtained. From typical S-P intervals of less than 1.5 seconds, a hypocentral distance of 5 or 6km was determined.

Occurrences of nanoevents--often having no resolvable P and S phases-- have been observed by us in many geothermal environments, from the area of Hot Springs, Virginia (Bollinger, 1974), to the eastern front of the Sierra Nevada in California. Because of their small amplitude and the fact that they are often seen on only one station, many observers probably discount them, or attribute them to very local noise sources-- rodents, cattle, frost, etc. In effect, however, such swarms may provide an important clue to the presence and behavior of an underlying geothermal system.

Instrumentation for microearthquakes

Ground motion resulting from seismic events is most frequently detected using seismometers composed of a coil and magnet (Figure 16a). Output from the transducers is transmitted either by cable to a nearby seismograph or by telemetry or telephone line to a central recorder. Vertical component seismometers are most commonly employed; however, horizontal component devices are often added to resolve earth motion into its three components and measure total energy.

The seismograph may be one of several types. The simplest is the familiar drum recorder, on which the amplified signal is traced on either smoked paper (using a stylus) (Figure 16b,c) or on white paper by means of an ink pen. They provide an immediate visible record of the recorded activity. Analog tape recorders have been used for more than 20 years, but they suffer from saturation or signal clipping when large or very close events come in. Digital recorders overcome this problem but require additional circuitry for A/D conversion. All tape systems on-site require protection from extreme temperatures, and like the drum recorders, require visits every day or so for record changing and possibly battery replacement.

The telemetered system transmits the analog or digital signals by means of a low-power voltage-controlled oscillator and transmitter to a central recorder. Data from multiple stations are recorded on multi-channel tapes or on drum recorders, usually installed in a truck. Because of their high transmission frequencies, these systems are limited essentially to line-of-site wireless links that result in serious constraints in network configuration. In most geothermal areas, topography is appreciable, so that to comprehensively cover the area, relay links are employed, or supplemental autonomous seismographs are placed in canyons or behind hills, where telemetry fails to reach.

Recently, event recorders have become available for long-term monitoring, obviating the need for continual maintenance and considerably reducing survey cost. These record and erase continually on an endless loop tape or in memory, until a signal of sufficient amplitude or an event from two or more other stations of the array is detected, in which case the record is dumped into a storage unit (tape or memory) for that particular recording cycle. Thus only the events matching the detection criteria are preserved, along with timing. Drawbacks to these

Figure 16. Microearthquake recording
station: a) Vertical-component
seismometer; b) Checking timing on
a MEQ-800 smoked paper drum
recorder; c) Resulting record for
one day, containing a regional
earthquake.
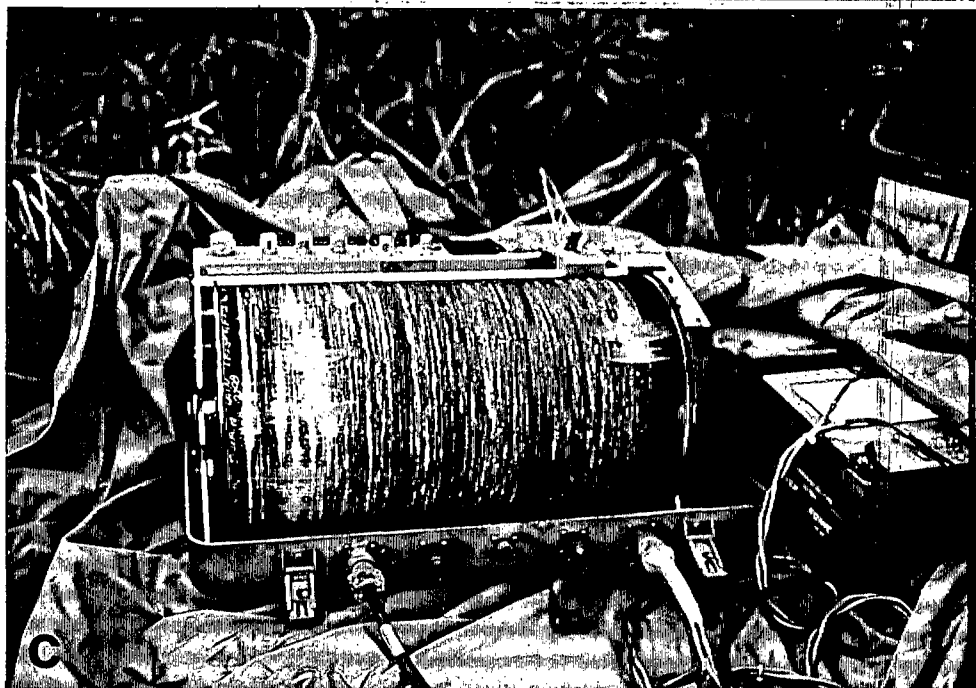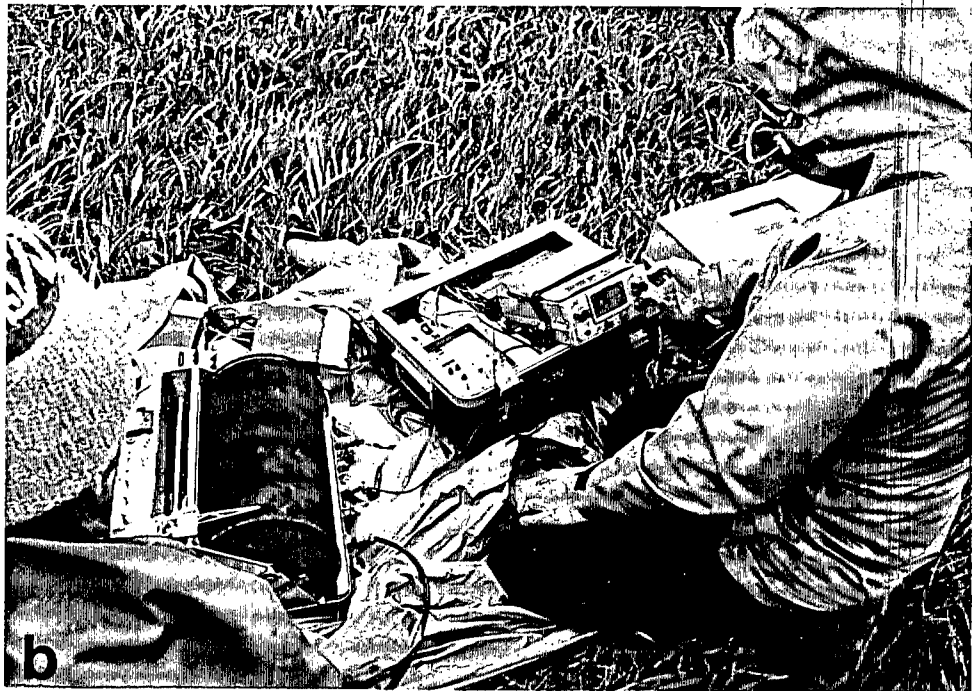
systems is their possible triggering by spurious noises and the fact that they may not preserve very low-amplitude events that may be particularly characteristic of geothermal seismicity.

Timing for all of these systems is generally initiated by radio communication from any of several time standards, such as radio station WWV operated by the National Bureau of Standards. The signal may be encoded directly on tape, but more commonly is used to trigger and synchronize a clock within the seismograph. Alternatively a portable clock is set by WWV and carried around to the individual sites.

When the records are processed, events of significance must be timed and tabulated. When multiple records are obtained on a common playback chart, it becomes an easy task to recognize earthquake arrivals. Modern processing techniques now permit automatic correlation and recognition of common events, greatly facilitating the compiling of data from zones of high activity.

Hypocenter determination

Epicenters and focal depths of microearthquakes can be computed by a variety of methods, depending on the number of arrival times available from a particular event and our knowledge of the velocity distribution with depth. As a first approximation, exact mathematical solutions can be obtained using arrival times from four stations and the assumption of a uniform half-space of constant velocity. If identifiable S-wave arrivals are employed, a hypocenter determination can be made using just three stations (cf., Appendix I). Utilizing more than four arrival times requires the application of a least-squares routine.

More complicated earth models are applied when information on the subsurface velocities is available or inferred. One of the simpler models is that of the constant velocity gradient, or linear increase of velocity with depth. If layering is suspected, as is the case with deeper sources, more complex iterative programs are employed, such as the HYPOLAYER series of the U.S. Geological Survey.

A comparative study of the various hypocenter computation systems is found in the report of Wechsler & Smith (1979).

References: Part I

BOLLINGER, G.A. & M.C. GILBERT (1974). A reconnaissance microearth-
quake survey of the Hot Springs, Virginia area. Seismological
Society of America, Bulletin 64 (6): 1715-1720.

BRUNE, J. & C.R. ALLEN (1967). A microearthquake survey of the San
Andreas fault system in southern California. Seismological Society
of America, Bulletin. 57: 277+.

CHOUET, BERNARD (1979). Sources of seismic events in the cooling lava
lake of Kilauea Iki, Hawaii. Journal of Geophysical Research 84
(B5): 2315-2330.

COMBS, J. & D. HADLEY (1977). Microearthquake investigation of the
Mesa geothermal anomaly, Imperial Valley, California. Geophysics
42 (1): 17-33.

COMBS, J. & Y. ROTSTEIN (1975). Microearthquake studies at the Coso
geothermal area, China Lake, California. United Nations Second
Symposium on the Development and Use of Geothermal Resources,
Proceedings. San Francisco, California. 2: 909-916.

EATON, G.P., CHRISTIANSEN, R.L., IYER, H.M., PITT, A.M., MABEY, D.R.,
BLANK, H.R., Jr., ZIETZ, I. & M.E. GETTINGS (1975). Magma beneath
Yellowstone National Park. Science 188: 787-796.

FERRICK, M.G., QAMAR, A. & W.F. ST. LAWRENCE (1982). Source mechanism
of volcanic tremor. Journal of Geophysical Research 87 (B10): 8675-
8683.

GUTENBERG, B. (1959). Physics of the Earth's Interior. New York,
Academic Press Inc., 240p.

HAGIWARA, T. & T. IWATA (1968). Summary of the seismographic observa-
tions of Matsuhiro swarm earthquakes. Earthquake Research Institute,
Bulletin 46: 485.

HAMILTON, R.M. & L.J.P. MUFFLER (1972). Microearthquakes at The
Geysers, California, geothermal area. Journal of Geophysical Research
77 (11): 2081-2086.

IYER, H.M., OPPENHEIMER, D.H. & T. HITCHCOCK (1978). Teleseismic P-
delays at the Geysers-Clear Lake, California geothermal region.
Geothermal Resources Council, Transactions 2.

JARZABEK, D. & J.COMBS (1976). Microearthquake survey of the Dunes
KGRA, Imperial Valley, Southern California. Geological Society of
America: Annual Meeting, Abstracts: 939.

JOHNSON, D.M. & J. COMBS (1976). Microearthquake survey of the
Kilbourne Hole KGRA, south central New Mexico. Geological Society
of America: Annual Meeting, Abstracts: 942.

KNAPP, R.B. & J.E. KNIGHT (1977). Differential thermal expansion of
pore fluids: Fracture propagation and microearthquake production in
hot pluton environments. Journal of Geophysical Research 82 (17):
2515-2522.

LANGE, A.L. & W.H. WESTPHAL (1969). Microearthquakes near The Geysers, Sonoma County, California. Journal of Geophysical Research 74 (17): 4277-4378.

MAJER, E.L. & T.V. McEVILLY (1979). Seismological investigations at The Geysers geothermal field. Geophysics 44 (2): 246-269.

MATUMOTO, T. (1971). Seismic body waves observed in the vicinity of Mount Katmai, Alaska, and evidence for the existence of molten chambers. Geological Society of America Bulletin 82: 2905-2920.

OKI, Y., OGINO, K., HIRANO, T., HIROTA, S., OGUCHI, T. & M. MORIYA (1968). Anomalous temperature encountered in the Gora hydrothermal system of Hakone volcano and its hydrological explanation. Kanagawa Prefecture, Hot Springs Research Institute, Bulletin 6: 1.

OKI, Y. & T. HIRANO (1970). Geothermal systems of Hakone volcano. United Nations Symposium on the Development and Utilization of Geothermal Resources, Pisa. Geothermics, special issue 2, 2: 1.

OPPENHEIMER, D. & D. EBERHART-PHILLIPS (1982). Induced seismicity at The Geysers, California. Society of Exploration Geophysicists: Annual International Meeting, Abstracts: 485. Dallas, TX.

PEARSON, CHRIS (1981). The relationship between microseismicity and high pore pressures during hydraulic stimulation experiments in low permeability granitic rocks. Journal of Geophysical Research 86 (B9): 7855-7864.

RICHTER, C.F. (1958). Elementary Seismology, W.H. Freeman and Company, Inc., San Francisco. 768p.

RYAN, M.P., KOYANAGI, R.Y. & R.S. FISKE (1981). Modeling the three-dimensional structure of macroscopic magma transport systems: Application of Kilauea Volcano, Hawaii. Journal of Geophysical Research 86 (B8): 7111-7129.

SCHAFF, S.C. (1981). Seismic monitoring and potential for induced seismicity at Roosevelt Hot Springs, Utah and Raft River, Idaho. Earthquake Notes 52 (1): 30.

SHEPARD, J.B., TOMBLIN, J.F. & D.A. WOO (1971). Volcano-seismic crisis in Montserrat, West Indies, 1966-67. Bulletin of Volcanology 35: 143.

SMITH, R.B., SHUEY, R.T., PELTON, J.R. & J.P. BAILEY (1977). Yellowstone hot spot: contemporary tectonics and crustal properties from earthquake and aeromagnetic data. Journal of Geophysical Research 82 (26): 3665-3676.

STAUDER, W. (1962). The focal mechanisms of earthquakes: Advances in Geophysics 9: 1-76.

STEEPLES, D.W. & A.M. PITT (1976). Microearthquakes in and near Long Valley, California. Journal of Geophysical Research. 81 (5): 841-847.

THATCHER, W. & J.N. BRUNE (1971). Seismic study of an oceanic ridge earthquake swarm in the Gulf of California. Royal Astronomical Society, Geophysical Journal 22: 473.

TOBIN, D.G., WARD, P.L. & C.L. DRAKE (1969). Microearthquakes in the Rift Valley of Kenya. Geological Society of America, Bulletin 80: 2043.

WARD, P.L. (1972). Microearthquakes: Prospecting tool and possible hazard in the development of geothermal resources. <u>Geothermics</u> 1 (1): 3-12.

WARD, P.L. & S. BJÖRNSSON (1971). Microearthquakes, swarms, and the geothermal areas of Iceland. <u>Journal of Geophysical Research</u> 76: 3952.

WARD, P.L., & K.H. JACOB (1971). Microearthquakes in the Ahuachapan geothermal field, El Salvador, Central America. <u>Science</u> 173: 328.

WARD, S.H., PARRY, W.T., NASH, W.P., SILL, W.R., COOK, K.L., SMITH, R.B., CHAPMAN, D.S., BROWN, F.H., WHELAN, J.A. & J.R. BOWMAN (1978). A summary of the geology, geochemistry, and geophysics of the Roosevelt Hot Springs thermal area, Utah. <u>Geophysics</u> 43 (7): 1515-1542.

WECHSLER, D.J. & R.B. SMITH (1979). <u>An Evaluation of Hypocenter Location Techniques with Applications to Southern Utah: Regional Earthquake Distributions and Seismicity of Geothermal Areas.</u> DOE Contract No. DE-AC07-78ET/28392. University of Utah: Department of Geology and Geophysics, Salt Lake City, UT. 131p.

Adak Microearthquake Survey and Results

At the invitation of the Earth Science Laboratory (E.S.L.) of the University of Utah Research Institute, Mincomp Exploration Resources participated in a microearthquake survey on Adak Island of the Aleutain chain, Alaska (Figure 17). The work was done as a sub-contract under Department of Energy Contract No DE-AC07-80ID12079.

The purpose of the project was to monitor seismicity around Adagdak Volcano and compute to a first approximation hypocenters of recorded events. Active faults, thus mapped, may provide conduits for hydrothermal fluids and aid in mapping a possible geothermal reservoir. Hot water from such a reservoir, whether of sufficient enthalpy for power generation or for space heating, could meet at least a part of the energy requirements for the Adak Naval facilities nearby.

Adak Island description

Adak is the largest island of the Andreanof Group, having a total area of 189km^2 (73mi^2) (Figure 17). It is approximately 46km (26mi) long in the north/south direction and 40km (25mi) in east/west extent; and is separated from Kagalaska Island on the east by the narrow Kagalaska Stait. The island falls between West Longitudes 176 and 177° and North Latitudes 51.5 and 52°; thus it lies 3° east of the International
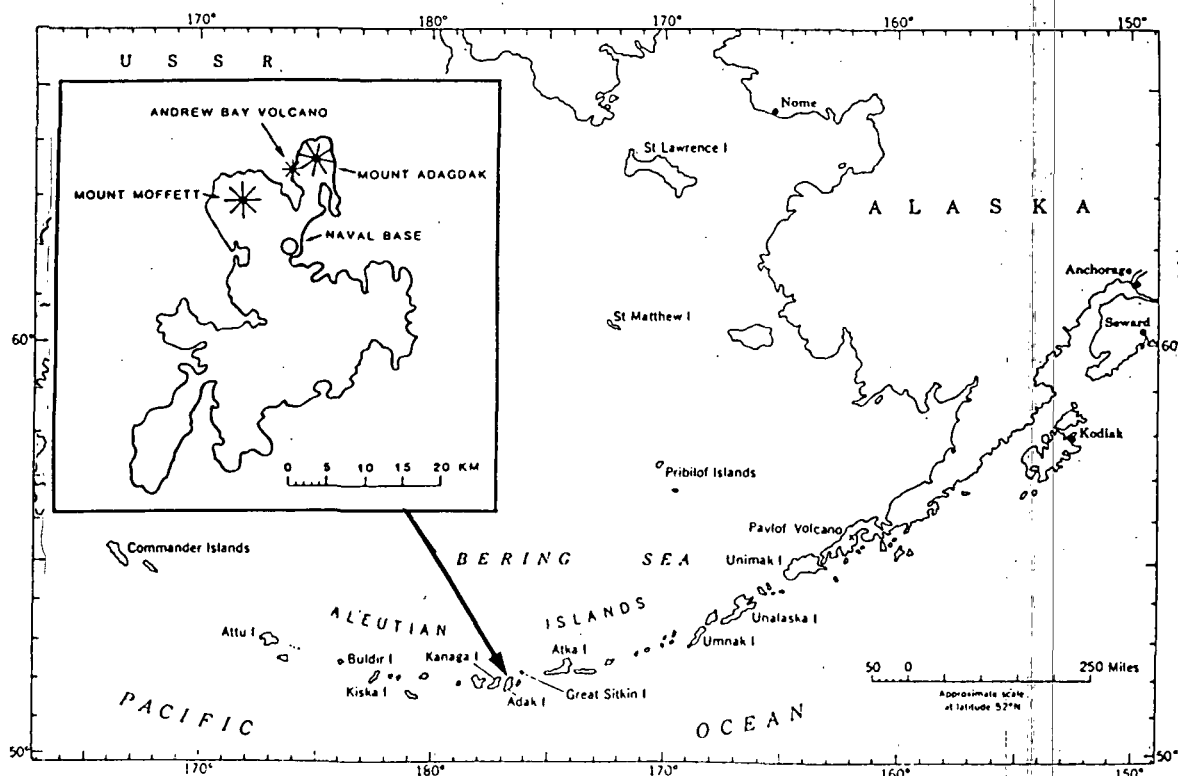

Figure 17. The Aleutian chain, showing Adak Island and the principal volcanoes.

Date Line, and slightly north of Prince Rupert, British Columbia.
Despite its southerly locale, the island is devoid of native trees, and
vegetation consists of alpine tundra. The island enjoys a maritime
climate, having summer average temperatures ranging between 5 and 13°C
and winter temperature between -2 and 5°C. Precipitation averages 173cm
rain or drizzle and 249cm of snow (68 and 98in., respectively).

The southern portion of Adak contains a physiography of glaciated
ridges, lake basins and fiords. The northern part is dominated by the
three basaltic volcanoes: Mt Adagdak, Mt Moffett and Andrew Bay volcano.
The eroded cone of Mt Moffett reaches 1182 (3876ft) in altitude;
Mt Adagdak attains 632m (2072ft). Kuluk Bay situated between the two
regions forms a sheltered harbor and the site of the Adak Naval installa-
tions.

Geologic summary

The Aleutian Islands lie along a convergent plate boundary that
is associated with active calc-alkaline volcanism and high seismicity.
A model of the Aleutian trench and subduction zone appears in Figure 18.
Adak, the largest island in the Andreanof group, is located near the
center of this magmatic arc. Like many of the surrounding islands, the
rocks of Adak Island can be divided into two contrasting units on the
basis of their geology and topographic expression. These units, desig-
nated as "early series" and "late series", are separated by a major
unconformity (Marlow, et al., 1973). On Adak Island rocks of the early
series belong to the Finger Bay volcanics--a thick sequence of intensely
altered and deformed basaltic volcanic rocks of Tertiary age that have
been intruded by plutons ranging in composition from gabbro to
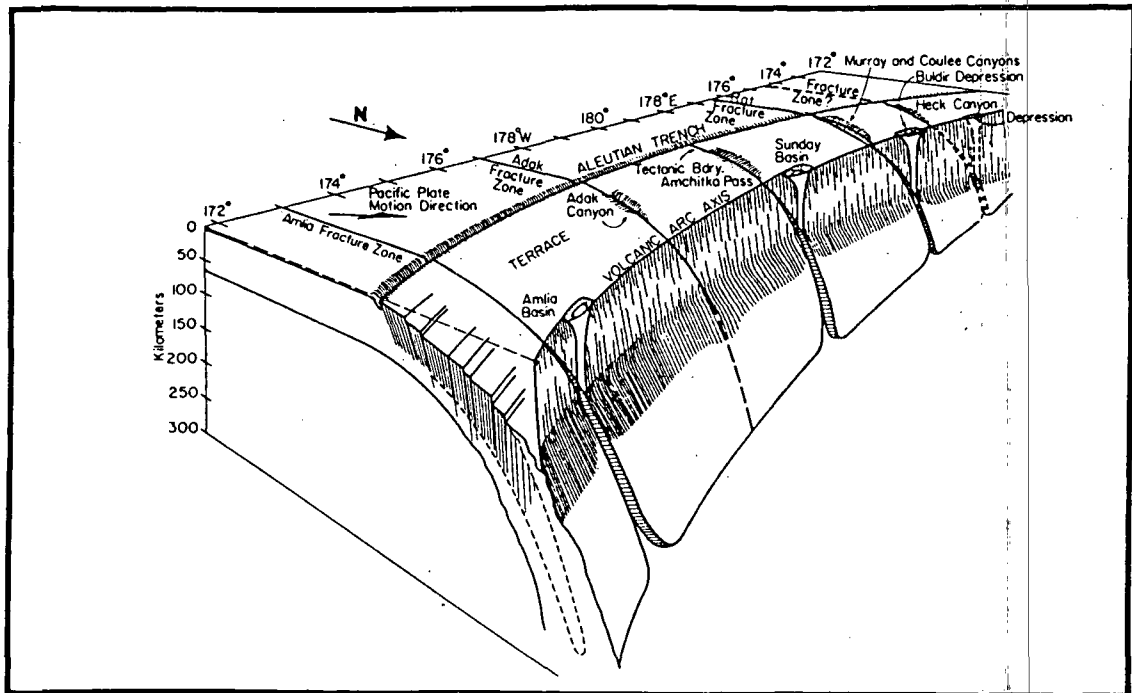granodiorite (Fraser & Snyder, 1956). These dense igneous rocks under-

Figure 18. Schematic diagram of the subducting Pacific plate
showing the major crustal features along the central Aleutian
arc (Spence, 1977).
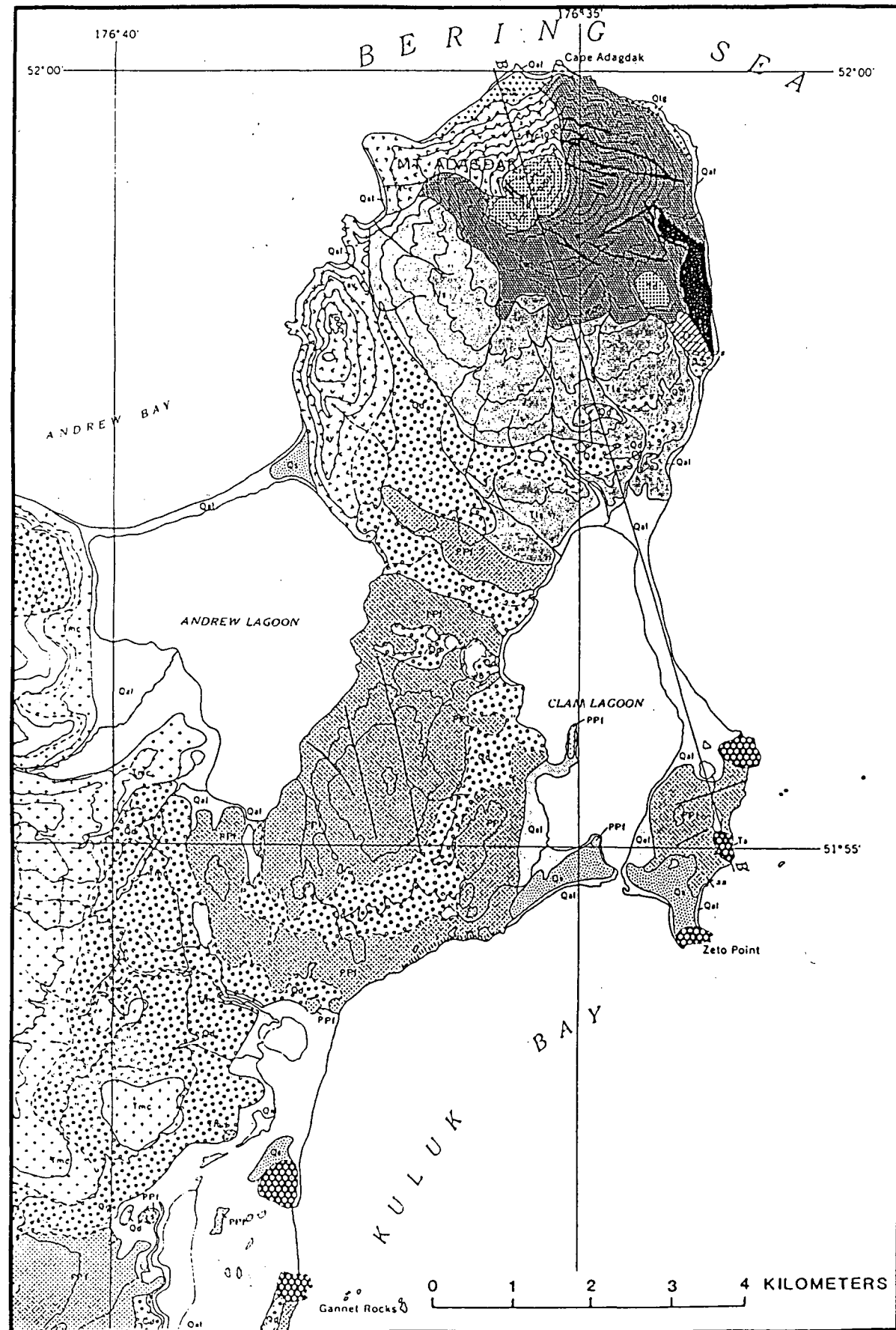
Figure 19. Geology of northeast Adak Island (from Coats, 1956).

EXPLANATION

A WIDESPREAD, THIN BLANKET OF WELL-STRATIFIED BASALTIC ASH AND PUMICE NOT SHOWN ON MAP

Sand dunes

Qal

Unconsolidated beach, delta, lagoon, and alluvial deposits

Marine terrace boulder gravel

Glacial drift
Including till, lateral moraines, and mudflows

UNCONFORMITY

QUATERNARY

Strike and dip of beds

Strike of vertical beds

Direction of glacial striae

Contact, dashed where inferred

Fault, dashed where inferred

NORTHEASTERN AREA
(NORTH OF ANDREW AND CLAM LAGOONS) MT. ADAGDAK VOLCANO

Basalt and andesite domes

Younger composite cone
Principally hornblende andesite tuff breccia, but includes some hornblende andesite flows

UNCONFORMITY

Older Composite cone
Principally hornblende andesite lapilli-tuff, but includes some hornblende andesite flows. Associated plug, Top, shown in section B-B'

UNCONFORMITY

Tis

Interbedded basalt lava flows and tuffaceous sandstone

UNCONFORMITY

Fossiliferous marine sandstone
Includes some conglomerate and shale

Bouldery conglomerate
Contains many giant talus blocks

Rocks of Andrew Bay volcano
Flows and tuff-breccia of olivine-, hypersthene-, and hornblende-bearing andesite

Andesite porphyry domes
Includes andesite porphyry, dacite porphyry, hornblende basalt porphyry, quartz-hornblende basalt porphyry, and hornblende-biotite basalt porphyry

UNCONFORMITY

Gabbro
Locally includes hornblende gabbro and augite-quartz syenite

Finger Bay volcanics
Basalt and hornblende basalt tuff, flow breccia, agglomerate, and basalt dikes and subordinate rhyolite tuff and quartz porphyry dikes

TERTIARY

PENNSYLVANIAN(?) OR PERMIAN(?)

-23-

lie the rugged mountians and broad rolling lowland areas in the deeply glaciated southern part of the island (Figure 19).

In the northern part of the island, rocks of the late series consist of interbedded late Tertiary to Quaternary lava flows, domes, and volcanogenic deposits associated with the remnants of three main eruptive centers. Several domes of andesite prophyry outcrop along the western margin of Kuluk Bay but their relationship to the main volcanoes remains unclear.

The remains of a heavily eroded andesitic volcano are now exposed in the steep-sided ridge that rises above the eastern shore of Andrew Lake. Following the erosion of this ancient volcano, volcanic activity was renewed resulting in the construction of two large composite cones-- Mt. Adagdak and Mt. Moffett. The early history of Mt. Adagdak is characterized by the eruption of thick basalt flows forming a broad shield volcano that was attacked by marine erosion and later capped with an andesitic composite cone. Volcanic activity ceased at this center following the extrusion of hornblende-andesite domes and flows within the summit crater.

The rocks near the summit and on the eastern flank of this volcano are cut by numerous recent faults that have an average trend of N65°W. The apparent throw of these faults indicates that the center of the mountain is subsiding within a graben-like structure.

The geologic history of Mt. Moffett is similar to that of Mt. Adagdak. Early eruptions in the form of basalt flows and domes produced a broad low volcano that was later capped with a steep basaltic tuff-breccia cone. Contemporaneous eruptions of basalt flows and scoria resulted in the formation of a fairly large parasitic cone on the northeast flank of the main composite cone. Volcanism ceased with the extrusion of basalt and andesite domes within the summit crater and on the flanks of Mt. Moffett.

The linear arrangement of Aleutian volcanoes suggests that major fault zones may be responsible for localizing volcanoes along the northern edge of the arc (Fraser & Snyder, 1956). The Andrew Lake volcano, Mt. Adagdak, Mt. Moffett and its parasitic cone all lie along a postulated northeast-trending fault zone. Great Sitkin, Koniuji, and Korovin volcanoes farther east are also believed to lie along this major crustal feature. Similarly, Kanaga, Bobrof, and Tanaga volcanoes to the west of Adak Island lie along a straight line, though on an offset, and slightly different trend. The change in the trend of these two volcanic alignments occurs over Adak Island.

Geothermal manifestations

The visual evidence of a possible geothermal reservoir on Adak consists of a group of sea-level hot springs situated on the west shore of Andrew Bay volcano (cf. Frontispiece and Figure 20, 21). Some of the pools mix with sea water, but discharge temperature of 68° C is reported in Miller, et al. (1977). They site geothermometer determinations by Don White of 187°C (Si O_2) and 196°C (Na-K-Ca); which if proven to be valid reservoir temperatures could possibly provide electric-power-

Figure 20. Adak Island
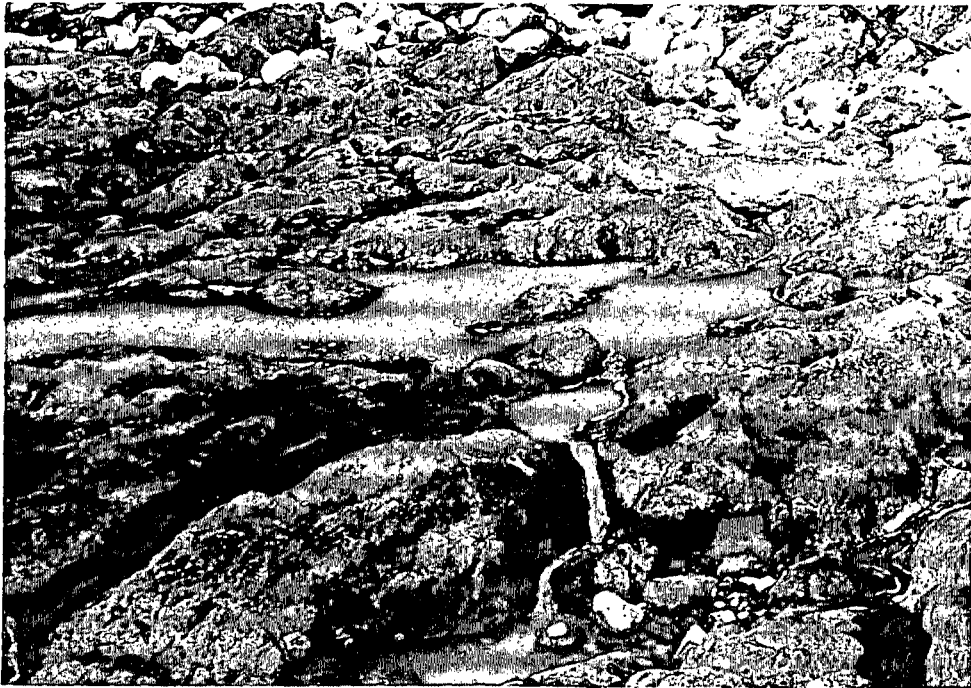 Hot Springs: sea water
 pool.

Figure 21. Hot water source pool.

generation capability.

While on Adak, we heard a rumor of fumarolic activity on the west
side of Mt Moffett, but this remains unverified. The next nearest
geothermal evidences are on Great Sitkin volcano, 35km to the northeast,
across Sitkin Sound. The volcano is active and issues steam from its
summit.

Previous microearthquake survey

A microearthquake survey was conducted during 9 days between 22
October and 1 November 1974 by Microgeophysics Corporation under contract
to the Colorado School of Mines (Butler & Keller, 1975). The survey was
performed with much the same instrumentation as in the present survey--
Sprengnether MEQ-800 smoked paper seismographs and Mark Products L4C
seismometers. Nine stations were installed around the west and south
sides of Mt Adagdak and around Andrew Lake. Their data were supplemented
by records from 5 NOAA stations then operating (Figure 22a).

Twenty-six local events having S-P times less than 4 seconds were
located and focal depths computed (Figure 22a). From their report it is
unclear whether they used a constant velocity model of either 4.5 or
5.5km/sec, or one of linear increase of velocity with depth approximating
a U.S.G.S. layered model. All of the epicenters fell offshore in Andrew
Bay and the Bering Sea. A plot of focal depths in cross-section (Figure
22b) suggests that the seismicity deepens seaward at a dip of 70° NW along
a strike of N60°E. When projected onto land, this fault trace passes
through both Mt Adagdak and Mt Moffett, as well as the Adak hot springs.
From a fault-plane solution they deduce the relative movement to be right-
lateral strike-slip with a small component of thrust. They produced
also a map of Poisson's ratio, in which values decreased from 0.29
on the west to 0.23-0.24 on the east, suggesting increased fracturing
at depth and to the west.

The interpretations of these data seem self-consistent and reasonable.
It is unfortunate that during the limited monitoring period no events
took place beneath the island. The present survey was more successful
in this respect and the preliminary findings seem to reinforce the land-
ward projections of Butler.

Other geophysical surveys

A variety of surveys have been conducted on Adak for the most part
addressed toward mapping a possible geothermal reservoir. At the time
of preparing this report we have on hand only portions of several manu-
scripts summarizing in the most general of terms the results, without
maps other than one locating the drillholes. Our deductions are summa-
rized here.

Aeromagnetic surveys reveal positive anomalies over Mts Adagdak
and Moffett, but slightly offset from the peaks, probably expressing
the distribution of volcanics rather than any geothermal properties. A
complete Bouguer gravity survey suggests a low-density mass expressed
by a 7mgal low on Mt Adagdak. This low is based on only one point at
the mountain top, so it warrants confirmatory points. Increased cover-
age on the southwestern flank suggests a possible gravity low in the
vicinity of Andrew Bay volcano. Gravity terrain corrections were
confined to a radius of 4km.
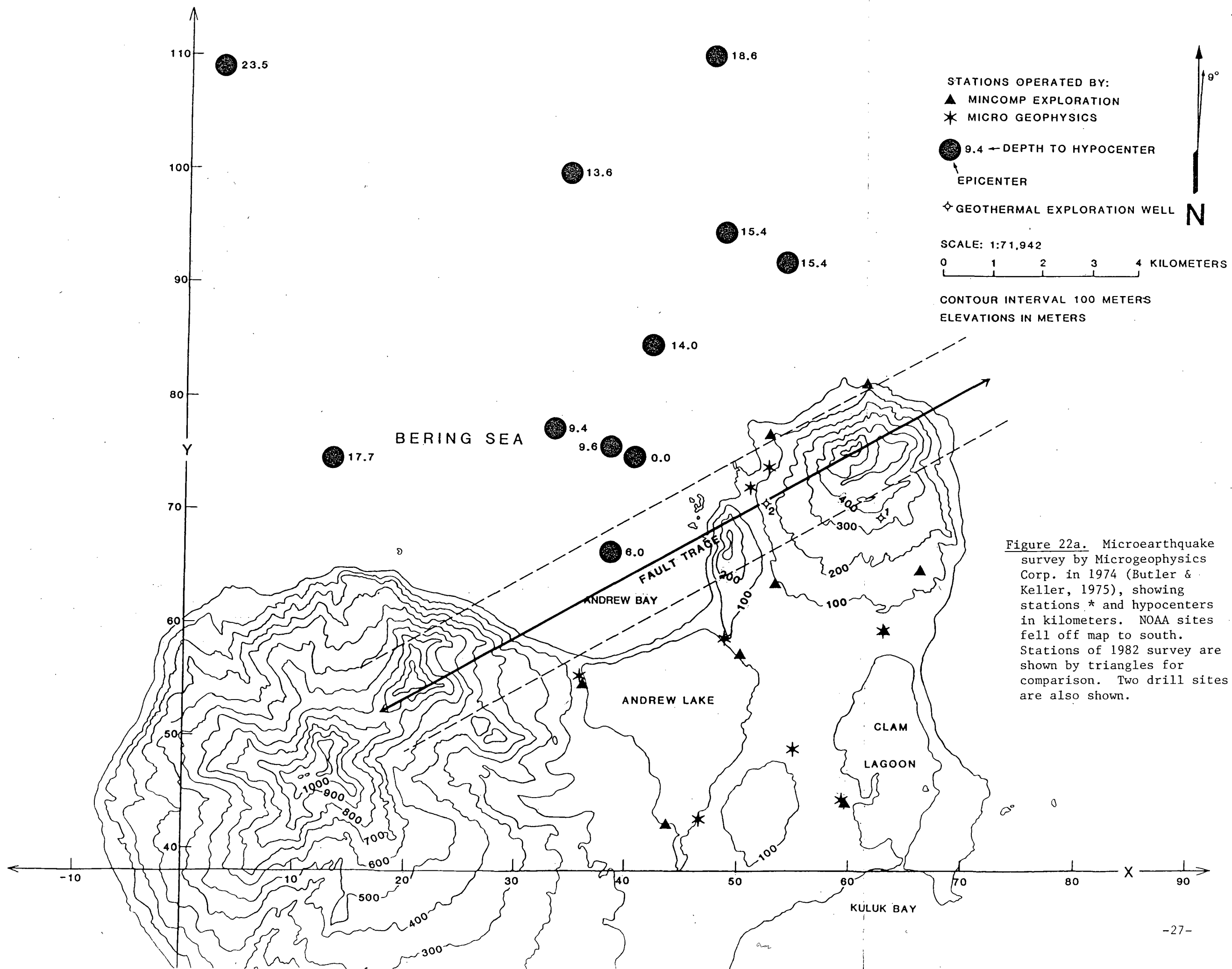
Figure 22a. Microearthquake survey by Microgeophysics Corp. in 1974 (Butler & Keller, 1975), showing stations * and hypocenters in kilometers. NOAA sites fell off map to south. Stations of 1982 survey are shown by triangles for comparison. Two drill sites are also shown.

STATIONS OPERATED BY:
▲ MINCOMP EXPLORATION
✳ MICRO GEOPHYSICS

● 9.4 ← DEPTH TO HYPOCENTER
↖ EPICENTER

◇ GEOTHERMAL EXPLORATION WELL

SCALE: 1:71,942

0   1   2   3   4 KILOMETERS

CONTOUR INTERVAL 100 METERS
ELEVATIONS IN METERS

BERING SEA

FAULT TRACE

ANDREW BAY

ANDREW LAKE

CLAM LAGOON

KULUK BAY

NW   SURFACE   SE

Z

FAULT PLANE

0 KM

1

2

3

4

5

SEISMIC EVENT
AT 23.5 KM

Figure 22b. 1974 Hypocenter
fault plane deduced by
Microgeophysics (Butler &
Keller, 1975).

-28-

A variety of electrical surveys have been run along the western and southern flanks of Mt Adagdak. A telluric low trends northeastward toward the mountain through Andrew Bay volcano. Schlumberger and audiomagnetotelluric (AMT) soundings in this same region show drops in resistivity at about 600m-depth from 500-1000Ωm 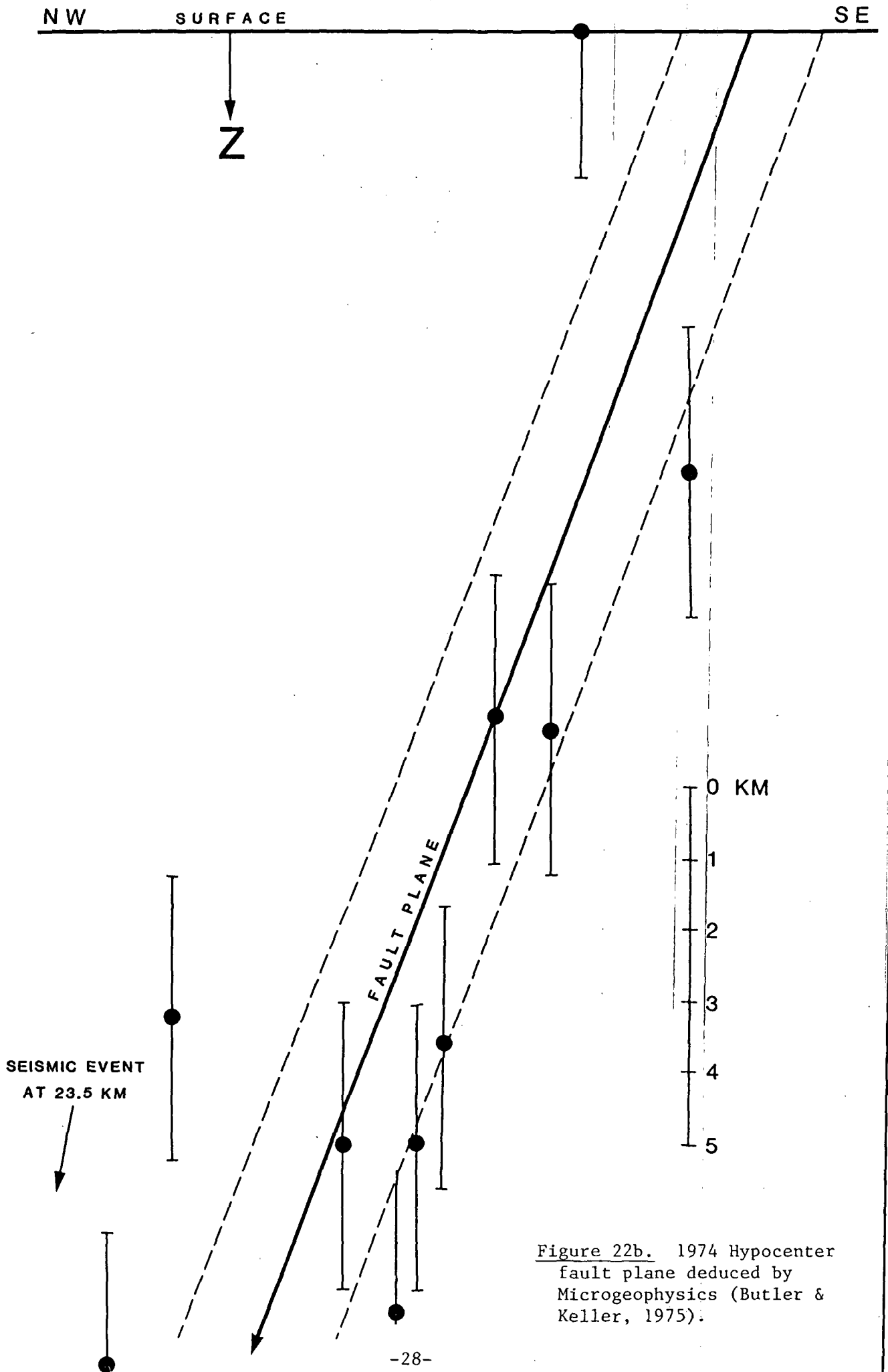on the surface to 5-10Ωm, decreasing downward. A limited bipole-dipole resistivity, and three magnetotelluric (MT) soundings proved inconclusive. Several self-potential lines were run along Andrew Bay and to the top of Adagdak. A suggestion of an SP low occurred in the vicinity of the other electrical lows, while the traverse up the peak revealed a strong negative correlation with altitude attributable to groundwater movement (Corwin & Hoover, 1979).

Three drillholes were attempted in 1977. The first was drilled over geophysical trends on the SE flank of Mt Adagdak. Drilling problems prevented penetration below 457m (1500ft) (cf. Figure 22a). A second hole drilled to 610m (2000ft) on the east flank of Andrew Bay volcano yielded a bottom-hole temperature of 66°C and a thermal gradient of 82°C/km. A third hole drilled in the area of Finger Bay, south of the Naval base was terminated at 91m (300ft) because of groundwater and drilling problems.

Survey operation

The work commenced 30 August 1982 with the procurement of seismograph equipment from the supplier in San Francisco. One MEQ smoked paper system was used for checkout procedures in the lab, eight others had been boxed for shipping* (cf. Appendix III for equipment details). The equipment was then air-freighted to Adak, via Anchorage. The survey crew, consisting of Claron Mackelprang and Steven Olson of E.S.L. and Walter Avramenko and Arthur Lange of Mincomp arrived in Anchorage on 31 August and flew to Adak on the following day. The seismographs were delayed in Anchorage awaiting space on Reeve's Aleutian Airways and did not arrive until the afternoon of 3 September. In the interim, the crew procured equipment and vehicles that could not be practically shipped, and reconnoitered for potential station sites selected by Mr. Lange. The seismographs were deployed during 4 and 5 September and recording commenced on the 5th. After the first few records were obtained, it was decided to move three of the noisiest stations to bedrock locations, where surf and wind noise would be minimized. In order to provide the proper geometric configuration for locating possible events under Adagdak volcano, two stations were backpacked to remote sites; Station 2 (Cape) to a bedrock promontory at Cape Adagdak, and Station 8 (Adagdak) to a sheltered ravine on the southeast flank (See Figure 32). The remaining stations could be serviced by vehicle. The latter stations were run at drum speeds of 120mm per minute requiring daily record changing; the remote stations were run at 60mm per minute, and needed to be serviced only every second day. Two persons--Mssrs. Avramenko and Olson--were thus able to mantain the nine stations. The sites were surveyed by Mr. Mackelprang with the assistance of the other crew members. Having completed their duties on Adak, Mssrs. Lange and Mackelprang flew out on 9 September. Mssrs. Olson and Avramenko main-

*Ten systems were supposed to have been supplied; however, upon unpacking at Adak, it was discovered that only 9 had been packed.

tained the equipment and made preliminary hypocentral determinations
using a Casio FX-720-P hand computer (cf., Appendix I for listing of
the program). The remote station at Cape Adagdak was retrieved on 3
October; the remaining stations were pulled in the following day. During
the 5th and 6th, the equipment was cleaned, packed and delivered to the
Adak airport for shipping. The crew left Adak on 7 October for Anchorage
and home.

Problems encountered

Aside from the delayed arrival of the equipment and the want of
the 10th unit, the survey ran quite smoothly. Early on, three station
sites were found to be noisy due to wind or surf noise and were moved
onto bedrock: Station 6 (Outhouse) was moved to Rocky Point; Station 4
(Andrew Lake) was moved to Lahar; and Station 5 (Tanks) was moved to
Clam Lagoon (Figure 32). The original sites were all within a few
hundred meters of the final sites. The internal clock in the seismograph
at Station 3 (Quonset) consistently lost about 900msec per day and could
not be corrected; hence, the timing error had to be linearly proportioned
for each record. The remaining clocks functioned within specifications.

Weather was not a serious problem in servicing the equipment;
however, wind, rain and surf whited out portions of the records,
particularly those on unconsolidated terrain and near the sea. The
vehicles rented from Northwest Maintenance were a constant trouble:
besides mechanical failures, tire failure averaged one case per day on
two vehicles. The brakes gave out on a vehicle while servicing Station
5 (Clam Lagoon), resulting in its running into the ravine below the
station. When the service company towed the vehicle out they dragged
it over the seismograph, putting it out of commission for about 5 days.
The instrument from Station 9 (Saddle) replaced the one at 5, since 5
was the site on which the best records were obtained.

Seismograph station descriptions

The final location of the seismographs of the present survey are
described here and referenced to the map, Figure 32. Photographs of
each of the sites appear in Figures 23-31 and coordinates, in Table 1.

(1) **Loran**: This station was located on the northwest flank of Mt Adagdak,
above an abandoned Coast Guard Loran station, at elevation 88.7m (291ft).
The geophone was buried in soil composed of layered volcanic ash, under-
lain by andesite tuff breccia at an undeterminable depth.

(2) **Cape**: Station 2 was situated on Cape Adagdak, north of the volcanic
peak on a wave-cut terrace at elevation 30.5m (100ft). The geophone
rested directly on bedrock composed of a fine-grained andesite flow with
well-developed platy cleavage.

(3) **Quonset**: The seismograph was placed inside an abandoned quonset hut
located in a small stream valley on the southern flank of Mt Adagdak.
The geophone was buried outside in organic-rich soil composed of
tuffaceous alluvium at elevation 26.5m (86.9ft). A thick blanket of
layered volcanic ash formed the walls of the stream valley.

(4) **Lahar**: This station was located on a bluff overlooking the north-
eastern shore of Andrew Lake. The geophone was buried on bedrock composed
of andesite-bearing tuff breccia belonging to the deeply eroded Andrew
Bay volcano, at an elevation of 13.9m (45.8ft).

(5) <u>Clam Lagoon</u>: This instrument site was located in a gully near the western shore of Clam Lagoon. The geophone rested on bedrock composed of light-grey hornblende andesite belonging to the Tertiary (?) Finger Bay Volcanics. Station elevation was 9.7m (31.7ft).

(6) <u>Rocky Point</u>: This station was emplaced at the base of a cliff on the southern shore of Andrew Lake. The geophone was buried in contact with bedrock composed of black porphyritic basalt belonging to the Tertiary (?) Finger Bay Volcanics, at elevation 6.1m (20.0ft).

(7) <u>Moffett</u>: The instrument site was located at the base of a bluff on the western shore of Andrew Lake at elevation 9.5m (31.2ft). The geophone was buried in soil composed of unconsolidated glacial till, overlain by layered volcanic ash. Basalt flows belonging to the composite cone of Moffett Volcano were exposed farther south along the lake shore.

(8) <u>Adagdak</u>: The instrument was placed at the head of a small gully on the southeastern flank of Mt Adagdak. The tundra at this locality is underlain by a fairly thick blanket of layered volcanic ash which in turn is underlain by lava flows belonging to an old basaltic shield volcano. The geophone was embedded in a firm layer of ash and lapilli at elevation 150m (492.5ft).

(9) <u>Saddle</u>: Station 9 was located in the valley between Mt Adagdak and the ridge belonging to the deeply eroded Andrew Bay volcano. The geophone was buried atop a thick blanket of soil composed of layered volcanic ash at elevation 99m (325ft).

| No.	Station	Grid Units X	Y	N. Lat.	W. Long.	Elevation ft.	m.
1	Loran	52.5	76.5	51°59'26.8"	176°36'58.6"	291.0	88.7
2	Cape	61.0	81.1	52°00'00.7"	176°35'17.8"	100.0	30.5
3	Quonset	62.9	59.2	51°57'19.3"	176°34'55.3"	86.9	26.5
4	Lahar	50.0	57.1	51°57'03.8"	176°37'28.2"	45.8	13.9
5	Clam Lagoon	59.5	44.0	51°55'27.3"	176°35'35.6"	31.7	9.7
6	Rocky Point	43.5	42.2	51°55'14.0"	176°38'45.3"	20.0	6.1
7	Moffett	36.0	54.5	51°56'44.7"	176°40'14.2"	31.2	9.5
8	Adagdak	66.0	64.5	51°57'58.4"	176°34'18.5"	492.5	150.0
9	Saddle	53.0	63.3	51°57'49.5"	176°36'52.6"	325.0	99.0
Origin of grid:		0.0	0.0	51 50'03.0"	176 47'21.0"	0.0	0.0

Table 1. Seismograph station coordinates.
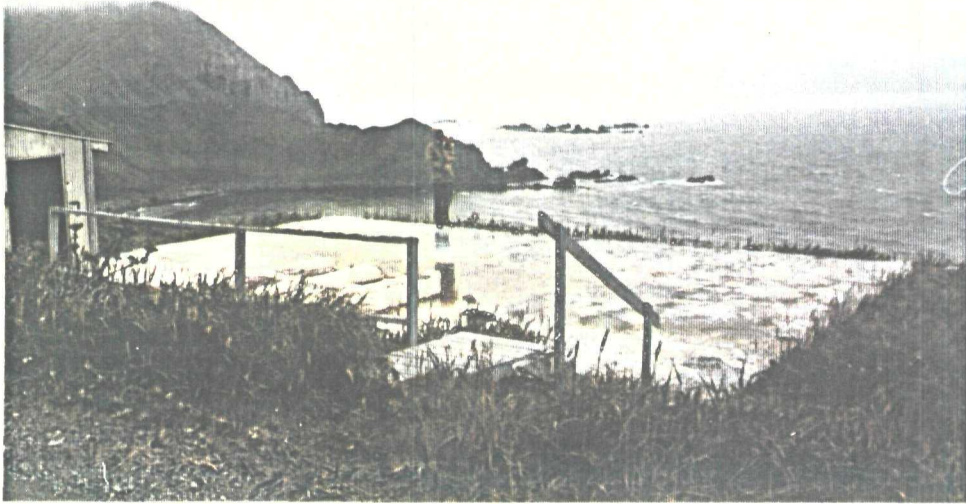
Figure 23. Station 1:
Loran

Figure 24. Station 2:
Cape Adagdak

Figure 25. Station 3:
Quonset

ADAK ISLAND, ALASKA

MICROEARTHQUAKE SURVEY:

Preliminary Hypocenter Determinations

by

Arthur L. Lange & Walter Avramenko

Erratum

Page 33: The photos of Figures 26 and 28 are to be switched:

Figure 26 should read "Station 6: Rocky Point"   and
Figure 28 should read "Station 4: Lahar".
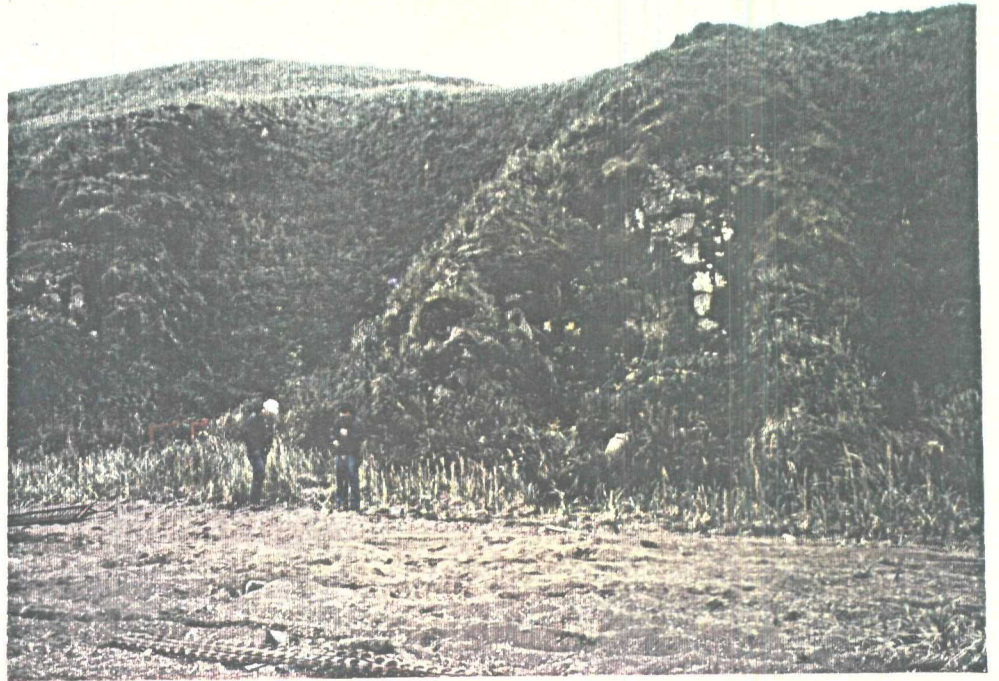
Figure 26. Station 4:
Lahar

Figure 27. Station 5:
Clam Lagoon

Figure 28. Station 6:
Rocky Point

Figure 29. Station 7: Moffett

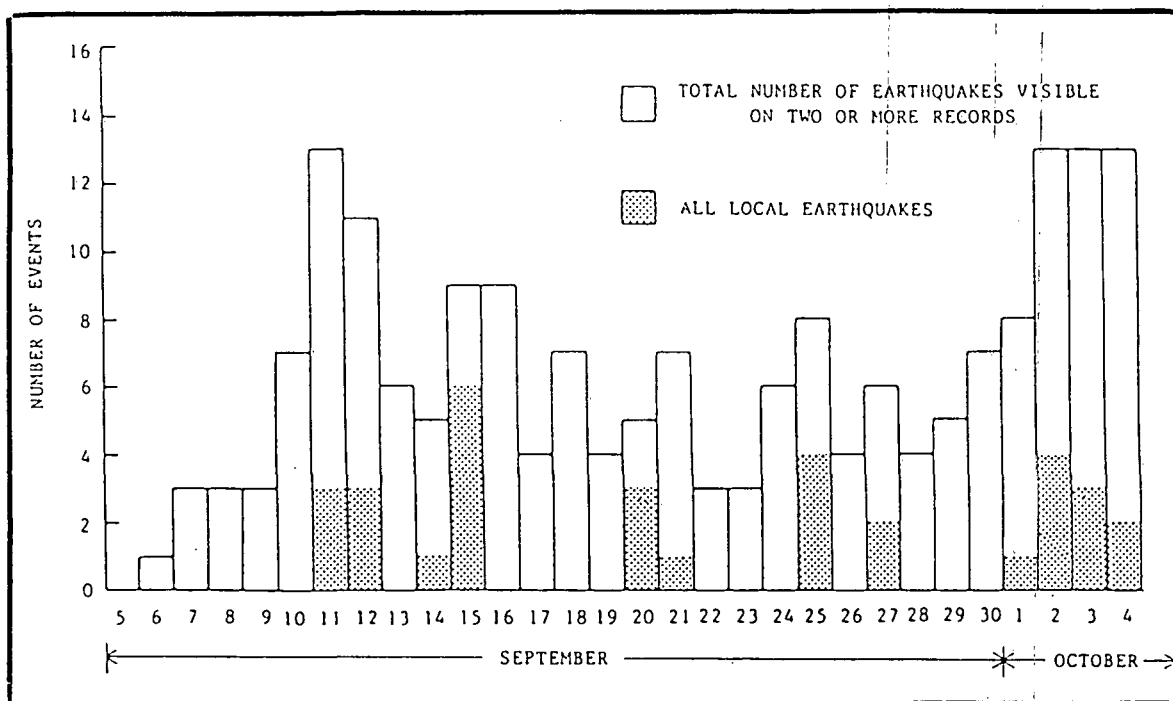Figure 30. Station 8: Adagdak

Figure 31. Station 9: Saddle

Figure 33. Frequency of occurrence of events seen on more than one record and of local events.

Frequency of occurrence of events

Recording began on 5 September and continued through 4 October 1982 (See Logistics Report, Appendix II), resulting in 30 days of recording. During that interval 190 events recognizable on two or more stations were detected (Figure 33). These include teleseisms, regional earthquakes as well as microearthquakes from local sources. Of the total, 33 events were considered local in origin--having S-P time intervals of less than 4sec (shaded columns in Figure 33). Of these, 31 were seen on 4 or more stations, and 24 yielded reasonable hypocenters and origin times based on a uniform earth of velocity 5km/sec. The remaining 7 events yielded only psuedo-hypocenters and origin times later than the arrivals--a condition discussed in the locating procedures of Appendix III. The principal facts and solutions for the local events are tabulated in the table of Appendix III.

No attempt was made to locate the distant or regional earthquakes that appeared on the records. Likewise, it was difficult to correlate swarms of very small microearthquakes, or nanoevents, that are seen on certain records (cf., below).

Distribution of located events

Figure 34 depicts the located events. Hypocenters were computed on the assumption of a uniform earth of constant seismic velocity of 5km/sec. Event numbers appear within the epicenter circle and the computed focal depths, outside. The size of the circle decreases with increasing depth, so as to give a perspective view of the seismicity.

The events were first determined while on Adak and recomputed later in the office. The lack of suitable maps and graph paper on the island led to the use of an improvised grid system in which 4.4 units constitute
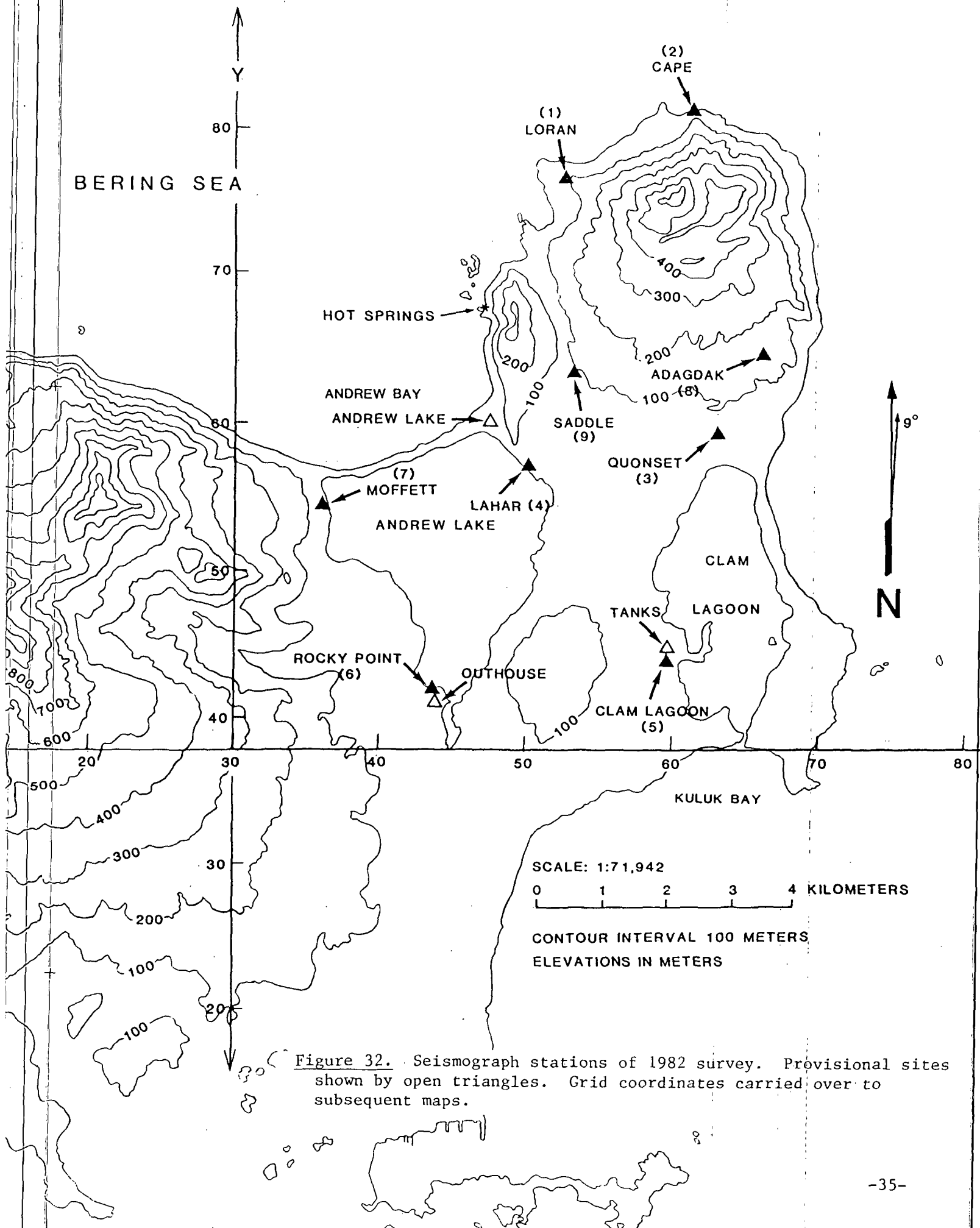
Figure 32. Seismograph stations of 1982 survey. Provisional sites shown by open triangles. Grid coordinates carried over to subsequent maps.
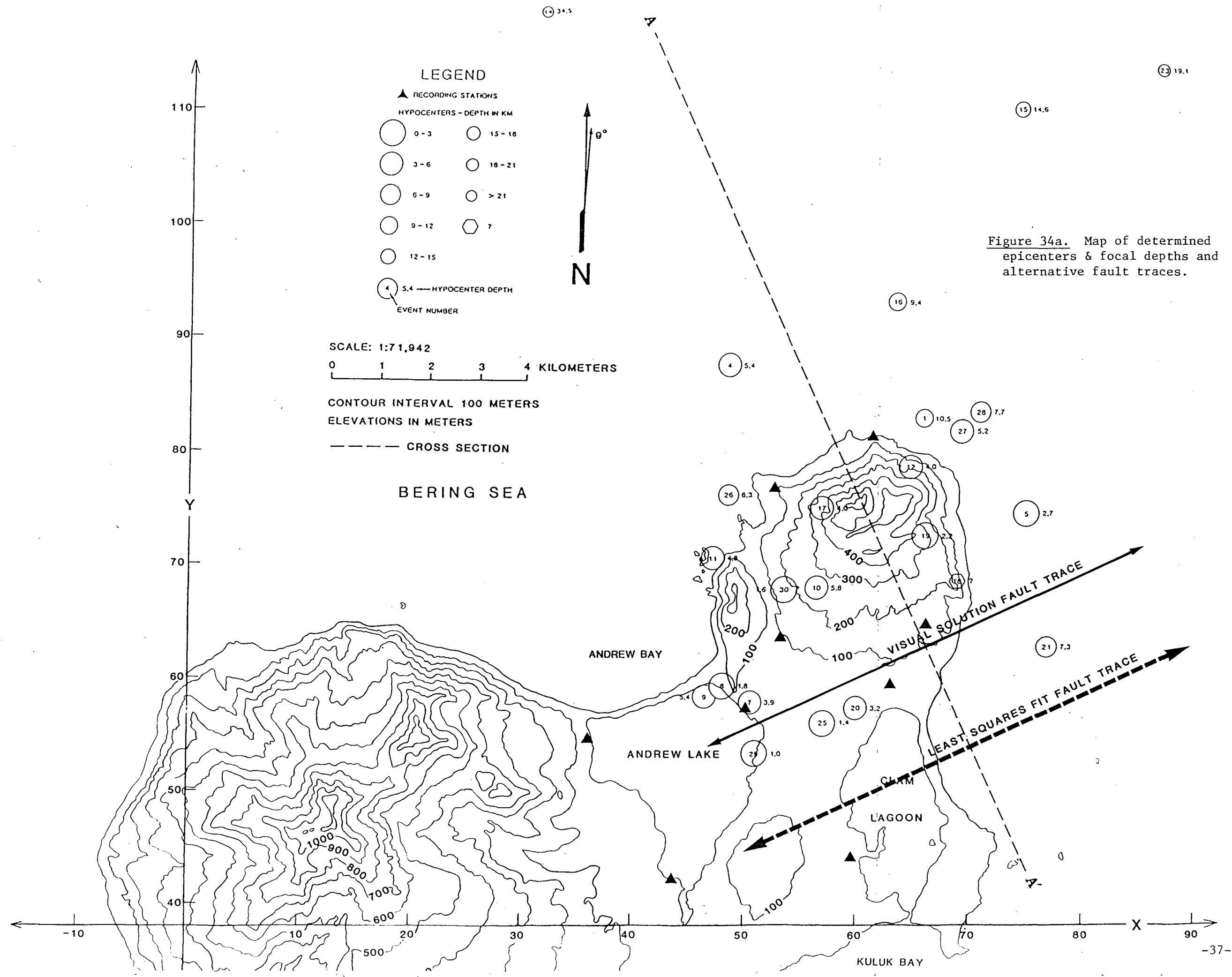
Figure 34a. Map of determined epicenters & focal depths and alternative fault traces.
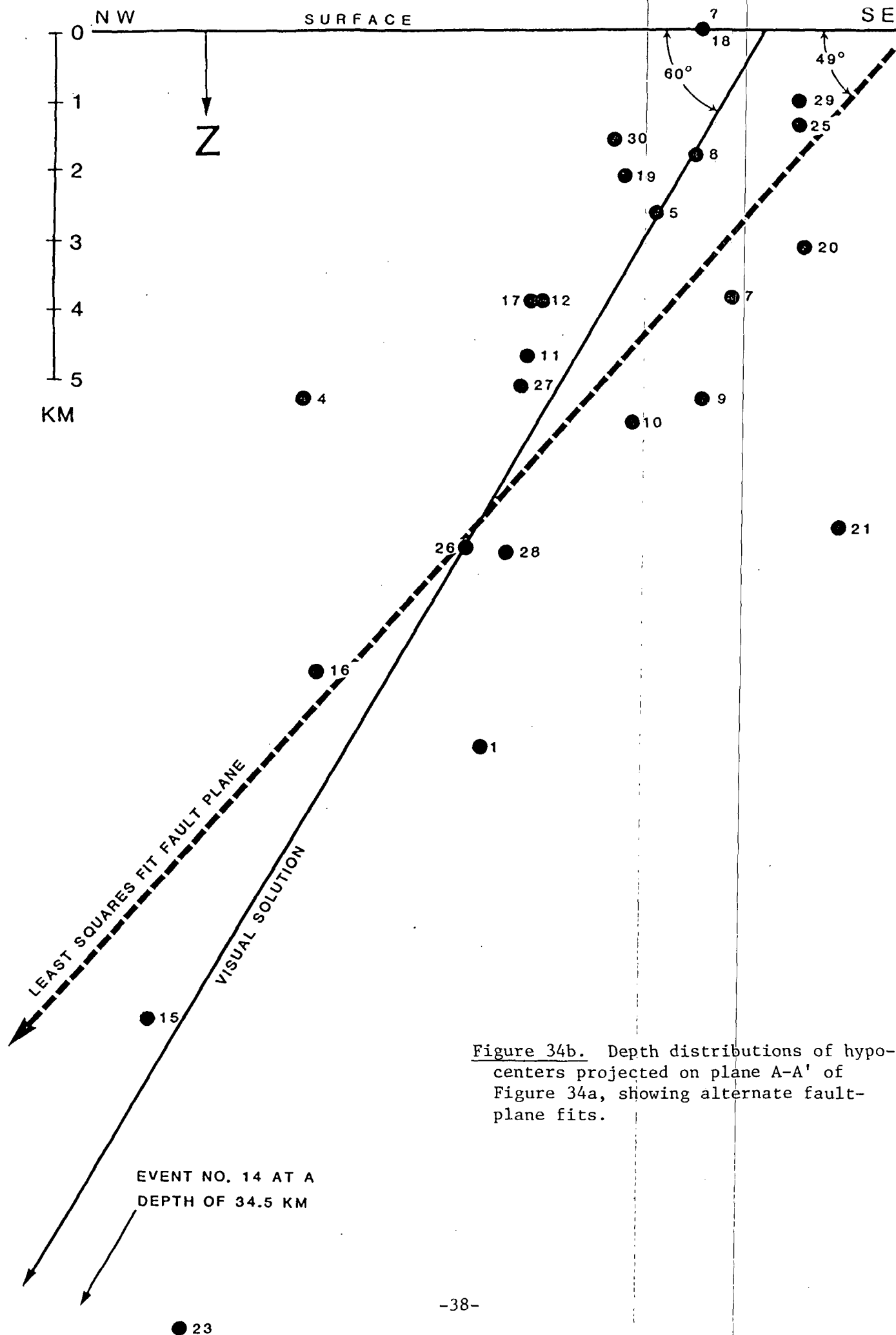
Figure 34b. Depth distributions of hypo-
centers projected on plane A-A' of
Figure 34a, showing alternate fault-
plane fits.

1km distance. This grid is shown on each of the succeeding maps along with the kilometer scale.

In the map we see that, unlike the 1974 survey, most of the activity took place around Mt Adagdak rather than under the sea. This distribution fits well the fault trace that Butler & Keller projected onto the land (Figure 22a). Their trace runs approximately NE/SW through Mt Adagdak and Andrew Bay volcano. When we examine the depths of the 1982 events (Figure 34b) we deduce a NNW-dipping structure similar to that found earlier (Figure 22b). When projected onto the vertical plane utilized by Butler & Keller (dashed line of Figure 34a), and compute a leastsquares plane through the hypocenters, we obtain a dip of 49° NNW and a surface trace falling SSE of the activity, passing through Clam Lagoon and the southern tip of Andrew Lake. An alternative visual solution displaces the trace approximately 2km to the NNW, with a dip of 60°, more in line with the 70° dip computed from the 1974 events.

The effects of different velocity assumptions were investigated in the case of 4 typical events: Nos. 1, 4, 11 and 19. Epicenters and depths resulting from velocities of 4, 5 and 6km/sec are plotted in Figure 35. Depths are extremely sensitive to velocity changes; however, the epicentral locations varied by less than a kilometer. Thus, the adoption of a higher velocity in the calculations would result in a steeper-dipping fault, and would move it further to the NNW.

Additional sensitivity analysis was performed, using a station elevation correction. From Table 1, we see that Stations 8, 9 and 1 were considerably higher than the others (150, 99 and 89m A.S.L., respectively), so that delays in arrival times might be expected. As a result of assigning a 3km/sec-velocity to the material above sea level, the epicenter displacements for Events 4, 5, 12, 17 and 26 shifted as in Figure 36, and changed in depth. We conclude that in a final analysis, elevation corrections should be applied to the arrival times.

Swarm activity

Very tiny events (nanoearthquakes) were observed on several stations, sometimes independently and sometimes in conjunction, but they could not be located. They were particularly noted on Stations 5 and 6 (Clam Lagoon and Rocky Point), which were sited on bedrock. Possibly the favorable rock coupling resulted in higher sensitivity to the activity, or, on the other hand, these stations lay closest to the deduced fault traces. Such swarming is seen close in to geothermal targets in a number of places (cf., Combs & Hadley, 1977) as illustrated in Figure 15.

Artillery and pistol firing go on at several places within the station net. Artillery was seen on the records from Station 4, and pistol practise was seen on 3. Such activities, particularly during daytime hours, should be kept in mind when examining the records.

Geothermal significance

In Part I, it was shown that many geothermal areas exhibit seismicity within and surrounding the region of elevated temperatures, or along controlling faults. On Adak, seismic activity is prevalent and seems
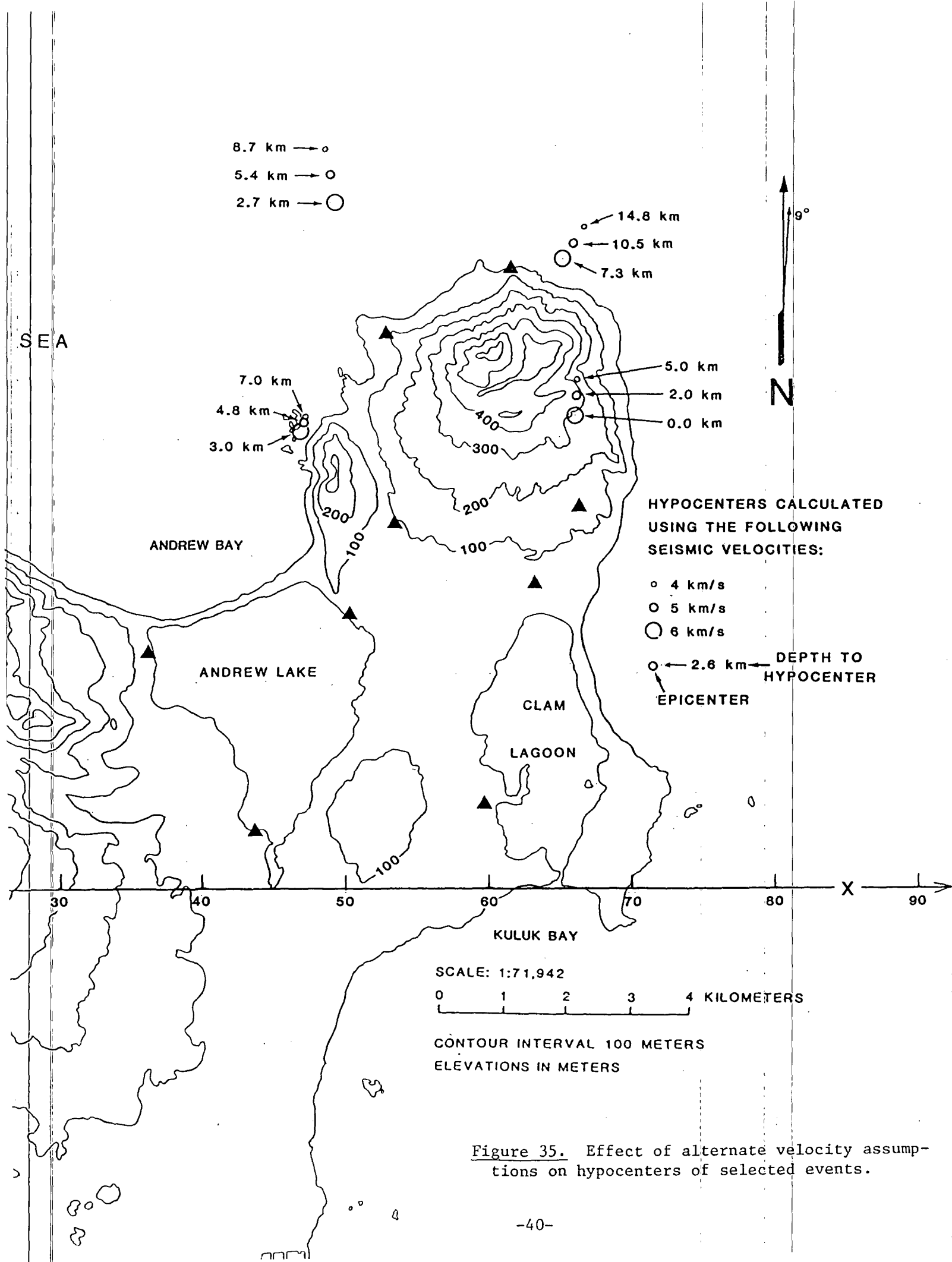
Figure 35. Effect of alternate velocity assumptions on hypocenters of selected events.
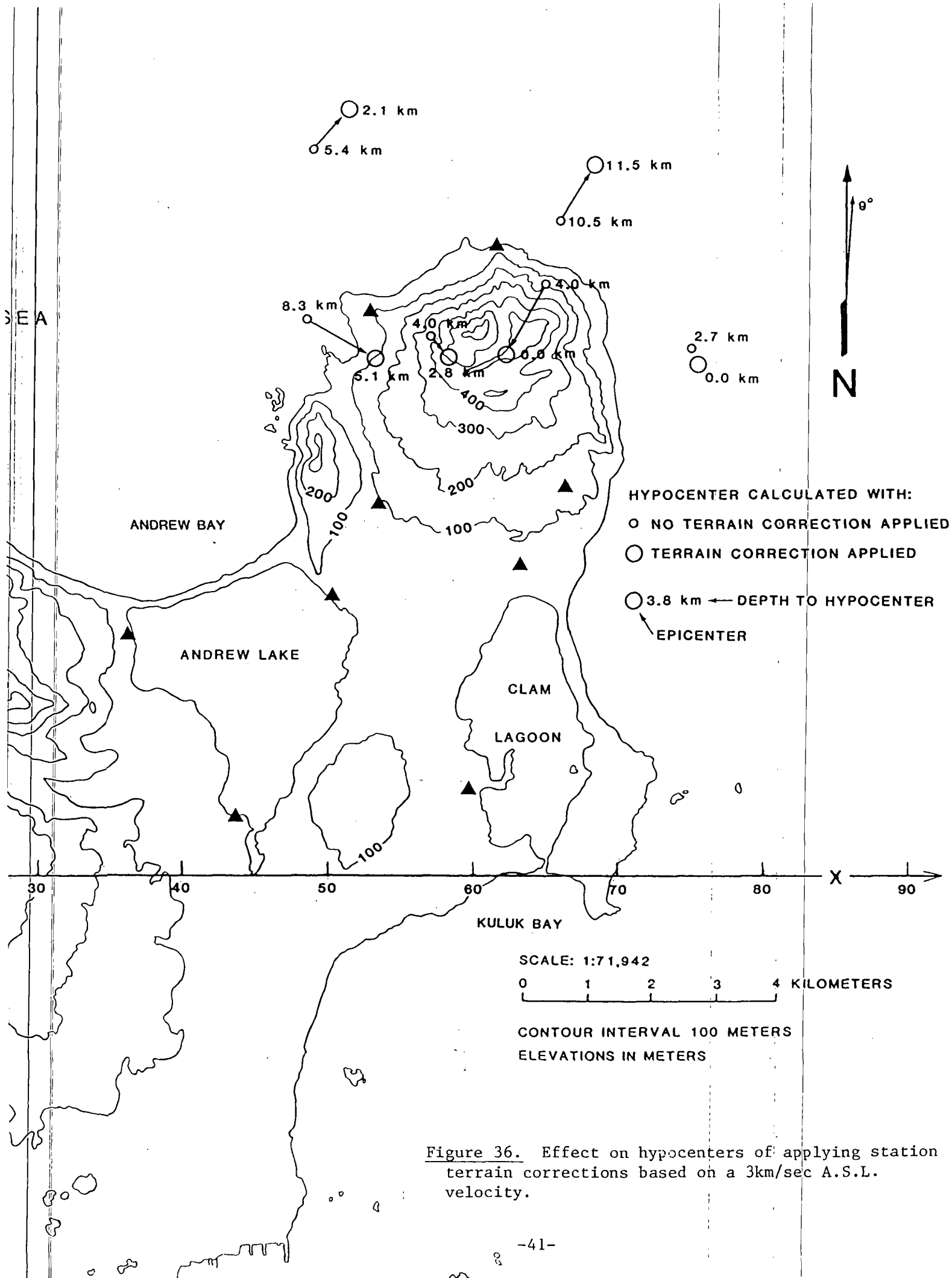
Figure 36. Effect on hypocenters of applying station terrain corrections based on a 3km/sec A.S.L. velocity.

to be distributed along a dipping fault plane beneath Mt Adagdak. Though the occurrence of Paleozoic outcrop in Figure 19 extends almost to our Station 7, seismic events to the SSE of the visually estimated fault, reinforce the argument for a more southerly surface projection of the structure--approximately through Clam Lagoon. Possibly more than one structure is active. The depth of the structure below the region of the hot springs and Andrew Bay volcano is then about 5km, but we caution that until more detailed analyses of events, including three-dimensional fault-plane solutions are performed, we can only say that the preliminary deductions are reasonable for a fault-controlled geothermal system. No doubt many fractures accompany the major structure, which could form a favorable zone of weakness and permeability in which a geothermal reservoir could have evolved and through which leakage could have migrated to the surface, as we see in the case of the hot springs.

Recommendations

It should be borne in mind that the scope of the present project included only the preliminary hypocenter determinations portrayed above. There remains much information in the existing data that should be unlocked before considering any additional passive seismic field work to refine the results. Some of the procedures that should be applied are the following:

1) Detailed scrutiny of the seismic records under magnification for higher resolution of timing and discovery of possible overlooked events.

2) Application of station terrain corrections to all events and adoption of an earth model that is more realistic than that of constant velocity.

3) Determination of hypocenters utilizing all available arrivals, rather than just the four required in the exact solution.

4) Fitting of the resulting hypocenters to a 3-dimensional fault structure.

5) Computation of fault-plane solutions based on first motions.

6) Analysis of frequency of events and estimation of Poisson's ratios.

7) Examination of regional events and teleseisms for possible P-wave delays.

If after performing these tasks, additional field monitoring seems warranted, it should be performed using at least some 3-component seismometers, high-resolution recording seismographs that permit filtering of noise and automatic correlations of events, and a telemetry system to minimize servicing of the stations. One or more calibrations shots would assist in determining terrain corrections and constructing the earth model.

Other techniques that could contribute to the mapping of a possible reservoir include a systematic self-potential survey to map locally ascending plumes of hot water across the area of interest, and carefully instrumented magnetotelluric soundings to determine the electrical

structure beneath the area of interest. Both the SP and MT results
should be modelled.

Conclusions

During 30 days of recording between 5 September and 4 October
1982, 190 discrete seismic events were recorded on two or more stations
of a nine-station network. Of the total, 33 were determined to be of
local origin, and of these 24 could be located.

The hypocenters of the located events delineate a fault plane
dipping north-northwestward toward the Bering Sea, beneath Mt Adagdak.
These determinations are based on a simple 5km/sec constant velocity
earth model. The surface projection of the fault appears to pass through
Clam Lagoon; however, pending more intense analysis of the data using
more realistic earth models and terrain corrections, these conclusions
should be regarded as very tentative.

A similar NNW-dipping fault plane was deduced from the 1974 survey,
in which all of the events occurred beneath the sea. Its projected
surface trace lies NNW of that deduced from the present survey.

The observed seismicity is favorable to the prospects of finding
a geothermal reservoir, and when higher resolution analysis is performed
on the data, the controlling structure can likely be clearly defined.
This structure and its attendant fracture system, could provide the
necessary permeability for the circulation of hot waters within the
upper several kilometers of the surface.

We recommend that more complete analysis of the existing data
be performed before consideration is given to follow-up passive seismic
work. Meanwhile, a high quality magnetotelluric survey and a systematic
self-potential survey should be performed and their results modeled
for the purpose of mapping electrical structure and possible ascending
hot waters.

Acknowledgements

References, Part II:

BUTLER, D.L. & GEORGE V. KELLER (1975). Exploration on Adak Island, Alaska. Appendix B of Grose, L.T. & G.V. Keller (1975). Geothermal Energy in the Pacific Region, Manuscript. Office of Naval Research, Anchorage.

COATS, R.R. (1956). Geology of northern Adak Island, Alaska. U.S. Geological Survey, Bulletin 1028-C: 45-67.

COMBS, J. & D. HADLEY (1977). Microearthquake investigation of the Mesa geothermal anomaly, Imperial Valley, California. Geophysics 42 (1): 17-33.

CORWIN, R.F. & D.B. HOOVER (1979). The self-potential method in geothermal exploration. Geophysics 44 (2): 226-245.

FRASER G.D., & G.L. SNYDER (1959). Geology of southern Adak Island and Kagalaska Island, Alaska. U.S. Geological Survey, Bulletin 1028-M: 371-408.

MARLOW, M.S., SCHOLL, D.W., BUFFINGTON, E.C. & T.R. ALPHA (1973). Tectonic history of the central Aleutian Arc. Geological Society of America, Bulletin 84: 1555-1574.

MILLER, T.P., HOOVER, D.B., SMITH, R.L. & CARL LONG (1977). A Case History of Geothermal Exploration on Adak Island, Alaska. Manuscript, U.S. Geological Survey.

SPENCE, W. (1977). The Aleutian Arc: Tectonic blocks, episodic sub-duction, strain diffusion, and magma generation. Journal of Geophysical Research 82 (2): 213-230.